Jack of All Trades, Master of Some, a Multi-Purpose Transformer Agent

Quentin Gallouédec[1,2], Edward Beeching[1], Clément Romac[1,3], and Emmanuel Dellandréa[2]

[1]Hugging Face
[2]Ecole Centrale de Lyon, CNRS, Universite Claude Bernard Lyon 1, INSA Lyon, Université Lumière Lyon 2, LIRIS, UMR5205, 69130 Ecully, France
[3]Inria (Flowers), University of Bordeaux, France

Abstract

The search for a general model that can operate seamlessly across multiple domains remains a key goal in machine learning research. The prevailing methodology in Reinforcement Learning (RL) typically limits models to a single task within a unimodal framework, a limitation that contrasts with the broader vision of a versatile, multi-domain model. In this paper, we present Jack of All Trades (JAT), a transformer-based model with a unique design optimized for handling sequential decision-making tasks and multi-modal data types. The JAT model demonstrates its robust capabilities and versatility by achieving strong performance on very different RL benchmarks, along with promising results on Computer Vision (CV) and Natural Language Processing (NLP) tasks, all using a single set of weights. The JAT model marks a significant step towards more general, cross-domain AI model design, and notably, it is the first model of its kind to be fully open-sourced[1], including a pioneering general-purpose dataset.

1 Introduction

Machine learning researchers have long aimed to develop versatile models that can adapt seamlessly to different domains. The recent success of Transformers (Vaswani et al., 2017) in NLP, CV, and to some extent in RL, has opened new avenues in this quest. In this paper, we attempt to extend the boundaries of this success by proposing a single, unified model capable of operating across a wide range of NLP, CV, and RL tasks using a single set of parameters. This effort not only seeks to challenge the conventional compartmentalization of AI tasks into distinct domains, but also aims to establish a more holistic approach to AI model design.

While combining visual and textual tasks has been well-researched, integrating RL tasks remains relatively unexplored and poses distinct challenges. RL tasks are inherently diverse and heterogeneous, making their combination among themselves and with other domains a highly complex exercise. This integration requires dealing with a landscape of different modalities, task complexities, and data volumes across domains and tasks. New questions that arise include: (1) How to design a model and learning method that effectively handles different modalities and data types (sequential decision-making and text-centric)? (2) How to formulate a learning objective that appropriately balances and harmonizes the different modalities, tasks, and domains without bias toward any particular domain or task? (3) How to design a learning strategy that can accommodate the different levels of complexity inherent in different tasks?

[1] `https://huggingface.co/jat-project/jat`

38th Workshop on Aligning Reinforcement Learning Experimentalists and Theorists (ARLET 2024).

These goals are concurrent and, to our knowledge, have only been addressed together by Reed et al. (2022) with the Gato model. Our contributions are characterized by three major advances: (1) Our model features an innovative structure optimized for sequential decision-making tasks. It uniquely assigns each timestep to a corresponding token embedding, resulting in a simpler design. This approach significantly expands the attention window in terms of timesteps compared to Gato (e.g., it is 19 times larger for Atari and more than 25 times larger for Meta-World). (2) In the spirit of open source, we release our code, dataset, and model to the research community. (3) We add observation prediction as an auxiliary task to our model. We demonstrate that this integration significantly contributes to learning a more efficient agent.

Ultimately, our JAT model achieves competitive results on the tasks studied, while being more than 6 times smaller than Gato and relying on a significantly lower training budget. As mentioned above, this new paradigm raises a number of open questions and paves the way for new research. We present a first milestone in this emerging framework and acknowledge the significant potential for improved results.

2 Related Work

2.1 Transformer for RL

Transformer models (Vaswani et al., 2017) are designed to model sequences and in particular sequences of words in natural language. However, sequence modeling problems span over a much larger set of domains than only NLP. Several efforts have been made to leverage these models for RL (Li et al., 2023). In this paper, we focus on modeling RL trajectories (i.e., sequences of observations, actions and rewards). Modeling such sequences with a Transformer was introduced by Chen et al. (2021) and the Decision Transformer (DT) model. In DT, a Transformer model is trained with offline RL to take sequences of transitions as input and predict the next action. In particular, Chen et al. (2021) proposed to use returns-to-go (i.e. the return from the current state) to condition actions' generation on both the previous observation and the desired return-to-go. While this has the advantage of explicitly modeling the relations between action selection and return, using the model at inference requires providing at every step a desired return. Liu & Abbeel (2023) proposed to extend this by using hindsight relabelling to better exploit sub-optimal trajectories. Zheng et al. (2022) also extended the DT approach by mixing offine pretraining and online finetuning. Finally, Lee et al. (2022) studied how the DT approach scales to a multi-task RL setup where a single policy is learned for multiple games. In terms of sequence structure, some discretize each dimension of the observation and action spaces separately (Reed et al., 2022; Janner et al., 2021; Chebotar et al., 2023), while others associate an embedding with each element of the sequence (Chen et al., 2021; Zheng et al., 2022).

Our work lies in this line of work as it also leverages Transformers to model trajectories. However, our approach (1) uses standard Behavior Cloning (BC) instead of conditional BC, relaxing the need to condition the agent by the return-to-go and (2) models a multi-task dataset in which sequences come from very different domains (e.g. control, Atari, visual question answering, see Section 3.2).

2.2 Multi-Modal Transformer

Apart from being widely used in NLP, Transformers also thrive in vision and vision-and-language domains. As one of the first works leveraging Transformers for vision, Dosovitskiy et al. (2021) introduced Vision Transformer (ViT), a Transformer model using image patches for recognition. Following this, a line of work aiming to train multi-modal Transformers using both text and images emerged, including works such as Flamingo (Alayrac et al., 2022), PaLI (Chen et al., 2023) or IDEFICS (Laurençon et al., 2023a). All these models imply the use of an image encoder allowing to obtain image tokens or embeddings that can be given to the Transformer alongside text tokens.

These models, typically generating text outputs, are trained for vision-and-language tasks like Visual Q&A. However, recent multi-modal Transformers focus on decision-making. For example, Jiang et al. (2022) trained a robot with Imitation Learning (IL) using multi-modal prompts to produce motor actions. RT-1 (Brohan et al., 2023b) and RT-2 (Brohan et al., 2023a) use expert demonstrations for real-world robots, with RT-2 building on RT-1 by directly outputting motor actions. Palm-E (Driess et al., 2023) leverages a pretrained Visual Language Model (VLM) for robotics tasks, producing sequences of text instructions executed by control policies.

Finally, our approach is largely inspired by Gato (Reed et al., 2022), which proposed to train a Transformer on both vision-and-language and decision-making tasks without relying on any pretrained model. The resulting model is therefore smaller than the ones leveraging large VLMs (e.g. Palm-E, RT-2) while still being able to perform both vision-and-language and decision-making tasks. In this paper, we first propose to build a dataset that resembles Gato's dataset except we only use open-source data sources and release all demonstrations as well as expert policies we used to obtain these demonstrations. Then, we also leverage a multi-modal Transformer along with IL for our model, but introduce several improvements, notably in the processing of sequential data and support for continuous values (see Section 3.1).

2.3 Multi-Task RL

The quest for a general agent has long been a goal of RL (Bellemare et al., 2013). However, most works have chosen to use a different neural network for each environment. Recent research has revived interest in this objective and explores it through several approaches.

One such approach involves directly extending online learning to multi-task environments (Espeholt et al., 2018; Yu et al., 2019; Song et al., 2020). These works highlight the potential for positive transfer in multi-task learning, meaning that learning across tasks can be mutually beneficial due to underlying commonalities. However, they also acknowledge the risk of negative transfer, where inter-task interference can impair training. Studies have investigated methods to limit this risk, such as that by Yang et al. (2020), which proposed refined gradient management techniques to mitigate these detrimental effects.

An alternative approach is policy distillation, which involves condensing the behaviors of expert agents into a singular, unified policy (Rusu et al., 2016; Parisotto et al., 2016). While these studies also report positive transfer across tasks (Rusu et al., 2016), they also identify instances of negative transfer. Subsequent research has focused on strategies to minimize this negative transfer (Teh et al., 2017). The reliance on the availability of policies to distill is a limitation. This constraint is notably addressed in (Chen et al., 2021), which proposes conditioning the distilled policy on the desired return thus allowing the use of any policy, including those of non-expert agents. This strategy has been adapted to the multi-task setting by Lee et al. (2022).

Despite the diversity of research in this area, most studies are limited to multi-task learning within a single domain, such as Atari or Meta-World, and thus involve semantically related tasks (although this is somewhat less true for Atari). The only notable exception we found is the Gato model (Reed et al., 2022), which learns a large number of domains in a single network. It is the closest baseline to our work.

3 Methodology

In this section, we introduce the JAT model, detailing our architectural choices that underpin its effectiveness and highlighting its ability to handle different modalities in both sequential decision-making and text-centric tasks. We present the associated dataset, which is notable for its groundbreaking diversity across domains and modalities. Finally, we discuss in depth the learning strategy used.

3.1 Model Architecture

3.1.1 Embedding Mechanism

The model is designed to handle two main categories of data: tasks involving sequential decision-making and text-centric tasks. In text-centric tasks, the model currently supports two modalities: text and image. Although the current version of the model supports image generation, we focus only on tasks that involve text generation. To ease reading, we will refer to it as *text-centric tasks* in the remainder of this paper. Each of these two categories requires a slightly different approach to the embedding process.

In both cases, the resulting sequence is truncated to match the maximum permissible input size of the inner Transformer model. Any truncated portion is not discarded; instead, it forms the basis of a new sample. This process may be repeated if necessary, ensuring that no valuable information is lost.

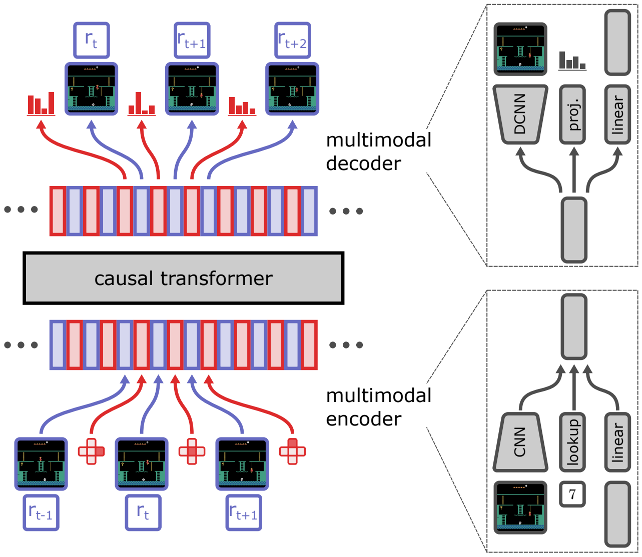

Figure 1: Architecture of the JAT network. For sequential decision-making tasks, observations and rewards on the one hand, and actions on the other, are encoded and interleaved. The model generates the next embedding autoregressively with a causal mask, and decodes according to expected modality.

Sequential Decision-Making Tasks For sequential decision-making tasks, the data comprises a sequence of observations, actions, and rewards. At the embedding stage, these sequences are processed to produce an interleaved sequence of observation embeddings (augmented with the corresponding reward) and action embeddings, denoted as $[\phi(s_0, 0.0), \phi(a_0), \phi(s_1, r_1), \phi(a_1), \ldots]$. Unlike DT (Chen et al., 2021) and Gato (Reed et al., 2022), each timestep is consistently associated with two embeddings: one for the observation and the other for the action, regardless of the modality. This enables JAT to better handle high-dimensional observations, and to provide a much wider, constant attention window in terms of timesteps. As an example, this multiplies the size of the attention window in terms of timesteps by more than 25 for Meta-World. The embedding method employed at a specific timestep is modality-dependent (with H the hidden size of the model):

- Continuous observation: The reward value is appended to the observation vector. This augmented vector is then padded to achieve a uniform length of 377, corresponding to the maximum augmented observation size in the dataset. The embedding vector is subsequently obtained by passing this padded vector through a linear layer with an output size of H. This layer is consistently used across all timesteps.
- Discrete observation: The observation consists of a vector of integers, each of which is encoded into a continuous vector of size H using a lookup table. Subsequently, a linear layer is applied to reduce the dimensionality to $\lfloor H/50 \rfloor$. Following vector flattening, another linear layer is applied, resulting in an output size of $H - 1$. Lastly, the reward is added to the resulting vector.
- Image observation: The input image is first resized to a uniform dimension of 84×84 using bicubic approximation, normalized, and padded to ensure 4 channels. The image encoder consists of a series of three blocks, each consisting of a convolutional layer, an instance normalization layer, and an attention layer. The output of the last block is flattened and passed through a linear layer, resulting in an embedding vector of size H.
- Continuous action: The process is similar to that of continuous observations, with the exception of the reward component. Notably, the linear layer is shared with the one used for continuous observations.
- Discrete action: In the case of discrete actions, the process is slightly different due to the nature of the input: a discrete action is represented by a single integer, as opposed to a vector of integers for discrete observations. The input is directly mapped to a continuous vector of size H using the same lookup table employed for discrete observations.

Text-Centric Tasks For text-centric tasks, each sample includes text, accompanied or not by an image.

- Image data: We employ the ViT architecture, as originally proposed by Dosovitskiy et al. (2021). The image is first cropped to its central square, and resized to 224×224. The image is then normalized and divided into non-overlapping patches of 16×16. Each patch is linearly embedded in a vector of size H.
- Text data: We use the GPT-2 tokenization strategy (Radford et al., 2019), utilizing a byte-pair encoding (Sennrich et al., 2016, BPE) specifically designed for unicode characters. This approach ensures comprehensive and granular tokenization. The tokenizer produces a vocabulary of 50,257 tokens. For efficient implementation, we use the Hugging Face integration (Moi & Patry, 2023). Each token is mapped to an embedding vector using a lookup table, where each unique token in the vocabulary is associated with a distinct vector. Notably, this lookup table is shared with the one employed for discrete values in sequential decision-making tasks.

When a sample includes both images and text, the embeddings are arranged so that the image embeddings precede the text embeddings. This specific order is essential for image captioning task because of the causal masking applied by the model's internal Transformer. The concatenated image-text embeddings form a unified representation for subsequent processing steps.

3.1.2 Transformer Architecture

The JAT model is based on a Transformer architecture using EleutherAI's implementation of GPT-Neo (Black et al., 2021). It takes as input the embedding sequence whose computation was described in the previous section. The model uses a dual attention mechanism whose design is inspired by the Longformer (Beltagy et al., 2020): global attention with a window size of 512 tokens for full context understanding, and local attention with a fixed window of 256 tokens. The Transformer's feed-forward components consist of 12 layers and 12 heads with an intermediate dimensionality of 8192 and a hidden size of 768. They are designed to be causal, meaning a causal mask is applied during training and inference.

3.1.3 Output Processing and Loss

The internal causal Transformer outputs a sequence of embeddings, each encoding the basis for predicting subsequent elements in different data modalities. As we predict multiple modalities within a single sequence, we use the appropriate decoders and corresponding loss functions for each modality. When an embedding encodes an image, we use a transposed convolutional neural network (Zeiler et al., 2010) for prediction. When an embedding represents a continuous vector, we use a continuous linear layer for prediction. For both image and continuous vector prediction, we compute the loss using Mean Square Error (MSE). When an embedding represents a discrete value, we assign scores to each discrete candidate using a linear projection layer and compute the loss using cross-entropy. Notably, we use the same projection layer for text tokens and discrete sequential values (like action for Atari and BabyAI). To compute the overall loss of the sequence, we average the individual losses computed for each element. For sequential decision-making task, we apply a weighting between the loss related to observations and the loss related to actions. We show in Section 4.3 that predicting the observations does help learning, and thereby solve one of the common open questions of (Chen et al., 2021) and (Reed et al., 2022).

3.2 Datasets

In this work, we have collected a wide range of datasets, classified into two main groups: sequential decision-making datasets and textual datasets. The former include a series of interaction sequences, each consisting of observations, actions and a subsequent rewards, generated by so-called expert agents, details of which are given in the Appendix B. The latter includes large corpora of textual data and image-text pairs. In order to promote the emerging field of general-purpose AI models, we have made these datasets, together with the expert agents and the full set of code required to generate them, available to the public as open resources in our Hugging Face repository, accessible at the following URL `https://huggingface.co/jat-project`. To the best of our knowledge, this compilation is unprecedented in terms of the variety of tasks and the volume of data, representing a valuable new contribution to the field.

3.3 Training

3.3.1 Overall Training Procedure

The model was trained for 250,000 steps. We distributed the training across 8 GPUs NVIDIA V100 using the Trainer from the Hugging Face Transformers library (Wolf et al., 2020) in conjunction with Accelerate (Gugger et al., 2022). This training lasted approximately 9 days. For practical reasons, each batch is made up of data from a single dataset. We use a constant batch size of 20 and accumulate over 2 steps, resulting in an effective batch size of 320. We use the AdamW optimizer with parameters $\beta_1 = 0.9$, $\beta_2 = 0.999$, and $\epsilon = 10^{-8}$. The learning rate starts at $5 \cdot 10^{-5}$ and linearly decays to zero throughout the training process.

3.3.2 Task-Specific Weight Adjustments

Each task presents a unique training challenge. To allow for balanced learning of all tasks, we introduced custom weight modifications. The choice of these weights is made heuristically. The learning would surely benefit from a more precise and systematic method for choosing these weights.

Sample Weight Some tasks required more updates for effective convergence. To allow proportionate progress of all tasks during learning, these tasks are sampled more frequently. Specifically, Oscar, Conceptual-Captions and Wikipedia was assigned a sample weight of 10.0 while other have a sample weight of 1.0.

Loss Weight Some control tasks require increased accuracy of actions. To allow for more strongly penalizing the error for these tasks, we assigned loss weights. In MuJoCo tasks, the loss weight is typically set at 10.0, except for the Pendulum task (20.0) and the Double Pendulum task (50.0). In Meta-World tasks, a uniform loss weight of 50.0 is used.

4 Experiments and Results

In this section we discuss the results of our experiments. First, we provide a brief overview of the model's performance on text-centric tasks. We then present the results of the sequential decision-making tasks, showing the different levels of mastery across the different domains within our study. Finally, we provide a comprehensive analysis highlighting the benefits of incorporating the prediction of the next observation as an auxiliary task during the learning process.

4.1 Text-Centric Tasks

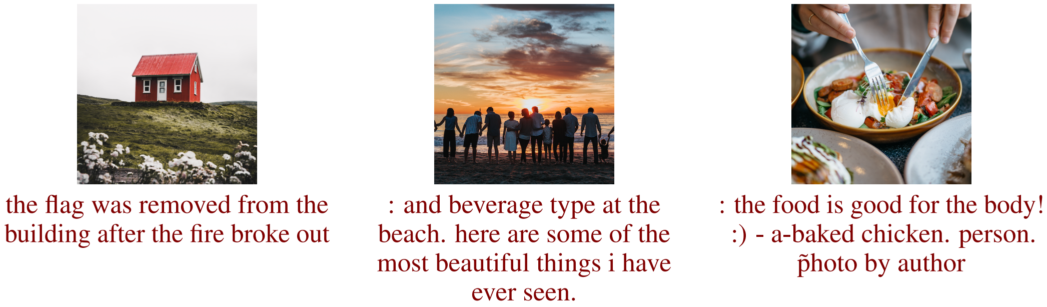

the flag was removed from the building after the fire broke out

: and beverage type at the beach. here are some of the most beautiful things i have ever seen.

: the food is good for the body! :) - a-baked chicken. person. p̃hoto by author

Figure 2: JAT image captioning examples. The theme is usually correct, although the relevance is sometimes limited.

We present a showcase of JAT's capabilities, with a particular focus on text completion and image captioning. It's important to note that JAT is much smaller and has a much lower training budget than the specialized models for these tasks. Therefore, instead of comparing it to these expert systems, we want to demonstrate its intrinsic capabilities. Figure 2 shows a selection of captioning results to illustrate how the model interprets and describes visual data. Additional examples are given in Appendix C. Figure 3, meanwhile, shows a series of text-based interactions that provide insight into its ability to complete text prompts. These examples were chosen to highlight the model's basic capabilities in these areas, providing a realistic view of its current state of development and potential for future enhancements. In addition, we provide a demos[2] for direct interaction and experimentation, allowing users to experience its functionalities.

INPUT	MODEL COMPLETION
The weather today is	a great time to the city of New York City. The city is a great place to stay in.
In the future, cars will	be able to drive cars to the market. The new car will be built in the new market for the new car.
My favorite book is	a book by the author of the book.

Figure 3: JAT text completion examples. The syntax is generally correct, the completion is on-topic, although the generated text may be wrong.

4.2 Sequential Decision-Making Tasks

We save checkpoints regularly during training. We evaluate each checkpoint on all the tasks on which it has been trained. Unlike Gato, the evaluation does not require any data to be used as a prompt. We show empirically in Appendix D that despite the absence of a prompt, and even in the worst case of our study, the agent still manages to identify the requested task. For each task, we collect 10 evaluation episodes and normalize by the average expert score of the dataset for this task. For the final checkpoint, we use 100 evaluation episodes. We then aggregate the results by domain. Figure 4 shows the evolution of the aggregate score for each domain during learning, and Figure 5 focuses on Atari, showing the human normalized score for each environment. The final results are presented in detail in Appendix A.

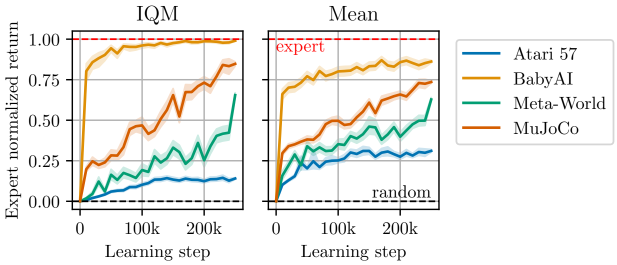

Figure 4: Aggregated expert normalized scores with 95% Confidence Intervals (CIs) for each RL domain as a function of learning step.

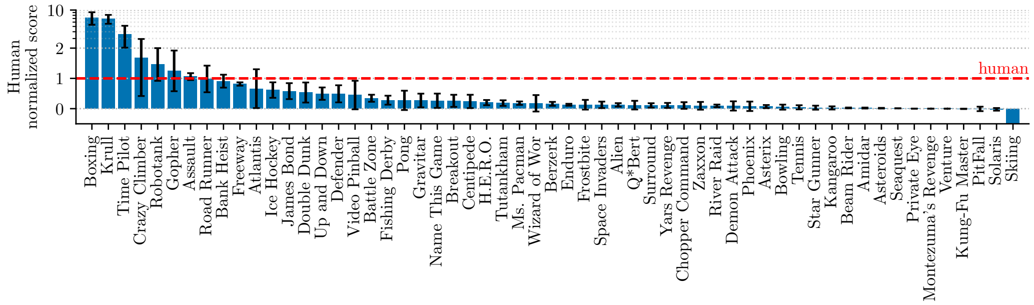

Figure 5: Human normalized scores for the JAT agent on the Atari 57 benchmark.

The final agent achieves a average expert normalized interquartile mean (IQM) of 65.8%, demonstrating the network's ability to effectively mimic expert agents across a wide range of tasks. The agent achieves 14.1% of the expert's score on the Atari 57 benchmark, corresponding to 37.6% of human performance, and exceeding the average human level in 21 games. For the BabyAI benchmark, JAT

[2] `https://huggingface.co/spaces/jat-project/text-completion`

achieves a normalized score of 99.0%. This score falls below 50% for only one task, namely Move Two Across S8N9. For this benchmark, however, there is no guarantee that the expert score can be achieved, since the bot used for dataset collection has access to the full state of the environment, while the interacting agents only have access to a partial observation. Finally, in the MuJoCo and Meta-World, JAT records scores of 84.8% and 65.5%, respectively. Although JAT reaches expert level for a fair number of Meta-World tasks, we note that some, such as basketball, have not been learned at all. Insofar as the action and observation spaces are identical for all tasks in this benchmark, these failures may be due to task indeterminacy, which we explore in more detail in Appendix D. Future research will have to confirm this hypothesis. We also note that some domains are mastered more quickly than others; in particular, BabyAI achieves a score of 90% after only 30,000 learning steps. We hypothesize that the high semantic similarity of the tasks enables a strong positive transfer, without however providing any proof of this. The Appendix A presents the final results in detail.

Although the results achieved are commendable, for a fair comparison we limit our benchmarking to Gato only, as it is the only truly comparable baseline. Reed et al. (2022) present results only for the 1.18 billion parameter version of Gato, which is 6 times larger than JAT. Its results are normalized to expert performance. Since we don't have access to the normalization parameters, we estimated scores for the random agents, which may not be exactly the same as those used by Reed et al. (2022), and used our expert scores for normalization, even though they obviously do not match those used by Reed et al. (2022). Therefore, comparisons of these normalized scores should be interpreted with great caution. On the Atari benchmark, JAT achieves an average normalized score of 31.1% outperforming Gato, which reports a score of 30.9%. For BabyAI, JAT achieves an average normalized score of 86.2%, close to the Gato score of 93.2%. Our study, however, is made with 39 tasks versus the 46 used in Gato's training, with the specific seven additional tasks in their study remaining unidentified. Since our evaluation includes all of the hardest tasks mentioned in their study, the seven missing tasks are likely to be easier, suggesting a harder test scenario in our study. For Meta-World, JAT achieves an average normalized score of 62.8%, which is below the 87.0% reported for Gato. On the MuJoCo benchmark, JAT achieves an average normalized score of 73.6%. While Gato's training doesn't use MuJoCo, it's worth noting that they use the DMC benchmark, which shares some similarities. For reference, on the DMC benchmark (Tassa et al., 2018), Gato achieves an average score of 63.6%.

4.3 Predicting the Observations Does Help

The model's main task is to predict the actions that maximize the sum of future rewards. Its ability to predict future observations is therefore not the main concern. However, can this ability contribute to better prediction of actions or accelerate the learning process? Two contrasting hypotheses emerge: firstly, learning to predict observations could serve as an auxiliary objective, directing the learning process towards a deeper understanding of the environment, which could lead to improved and faster learning. Conversely, this prediction learning could serve as a distracting objective: instead of excelling in action prediction, the model might only achieve moderate performance in both action and observation prediction. This could slow down the learning process, resulting in a lower overall performance score. Reed et al. (2022) choose not to predict the observation, but does not study the influence of this prediction on learning.

To answer this question, we use a loss function that combines observation loss ($\mathcal{L}_{\text{obs}}$) and action loss ($\mathcal{L}_{\text{act}}$), balanced by a weighting parameter κ. The function is defined as:

$$\mathcal{L} = \kappa \cdot \mathcal{L}_{\text{obs}} + (1 - \kappa) \cdot \mathcal{L}_{\text{act}} \tag{1}$$

We select a range of values for κ and train the model on a subset of 6 dataset tasks from different domains (Freeway, Pong, ButtonPressWall, WindowClose, Ant and DoubleInvertedPendulum). Figure 6 compares the results at the end of training for the different values of κ.

In our study of the κ coefficient and its impact on learning, we find an interesting balance. When set to the highest value in our range ($\kappa = 0.5$), the learning process seems to be somewhat hindered by the additional objective. On the other hand, at lower κ values, this added task of predicting observations doesn't significantly impact learning, leading to scores that are similar to the base score of $94.5 \pm 1.1\%$, which we get when predicting observations isn't part of the objective. The sweet spot appears to be around $\kappa = 0.005$. Learning to predict observations doesn't distract but actually improves the agent's learning efficiency, achieving an near-optimal score of $99.1 \pm 0.4\%$. This finding highlights that adding observation prediction into the learning process is beneficial, provided it's balanced correctly.

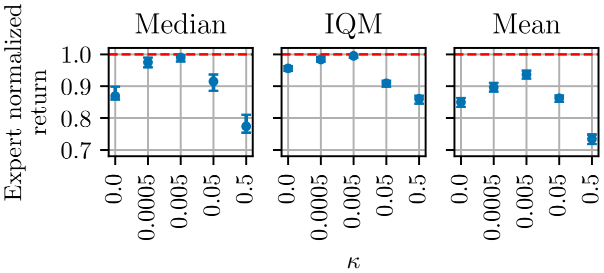

Figure 6: Aggregate measures with 95% CIs for the study on the influence of observation prediction learning for selected tasks. The results presented cover the selected range of κ values and are based on 100 evaluations per task. Optimal κ selection can significantly improve agent performance.

5 Conclusion

In this study, we introduce JAT, a novel multi-modal framework for general RL agents. JAT features the ability to handle diverse tasks of varying complexity using a single set of parameters. Its innovations include a new transformer-based structure that efficiently addresses sequential decision-making, CV, and NLP tasks. We also show that joint learning of observation prediction significantly improves performance in sequential decision-making tasks. We've open-sourced our training dataset, which includes a wide range of sequential decision-making data as well as extensive language and visual data. We believe that JAT represents an important and valuable step towards general-purpose RL models.

This study reveals several avenues for improvement. A primary challenge is the joint learning of tasks characterized by high heterogeneity. Our dataset features variations in size, task complexity, and accuracy requirements for optimal performance. Our current approach, which uses basic sample and loss weighting, partially addresses this challenge. A refinement of task sampling could potentially account for task difficulty, although quantifying *difficulty* remains a challenge. Another important challenge is imitation learning. While our current method relies on rudimentary behavioral cloning, the use of more advanced imitation learning techniques is likely to yield better results. In addition, improving the quality of expert data is a clear opportunity for improvement. For example, in the Asterix task, our model's expert score (3699.6) lags significantly behind the scores achieved by agents such as R2D2 (999,153.3) (Kapturowski et al., 2019). Using the best RL agent for each specific task could significantly improve the overall scores in our dataset, leading to better results when distilled for the generalist agent.

Broader Impact

What sets generalist agents apart is their ability to produce output in a wide range of modalities (textual, visual, virtual or physical control) for multiple applications. This versatility introduces a potential for cross-domain generalisation, although no work to our knowledge actually demonstrates this transfer. The theoretical risk is that such agents transpose behaviours from one domain to another in an inappropriate or undesirable way, and raises important ethical and safety questions. For example, translating aggressive actions in a virtual environment (which may be legitimate in the context of a game or film) into harmful behaviour in the real world. While the alignment of large language models (LLMs) with human values and preferences has been extensively studied (Ouyang et al., 2022; Rafailov et al., 2023; Azar et al., 2023), the application of these alignment strategies to the broader category of generalist models has not been examined in depth. The adaptation of existing alignment methodologies to the requirements of generalist agents is necessary to enable more reliable and secure models.

Acknowledgments and Disclosure of Funding

This work was granted access to the HPC resources of IDRIS under the allocation 2022-[AD011012172R1] made by GENCI.

References

Agarwal, R., Schwarzer, M., Castro, P. S., Courville, A. C., and Bellemare, M. G. Deep Reinforcement Learning at the Edge of the Statistical Precipice. In Ranzato, M., Beygelzimer, A., Dauphin, Y. N., Liang, P., and Vaughan, J. W. (eds.), *Advances in Neural Information Processing Systems 34: Annual Conference on Neural Information Processing Systems 2021, NeurIPS 2021, December 6-14, 2021, virtual*, pp. 29304–29320, 2021. URL `https://proceedings.neurips.cc/paper/2021/hash/f514cec81cb148559cf475e7426eed5e-Abstract.html`.

Alayrac, J., Donahue, J., Luc, P., Miech, A., Barr, I., Hasson, Y., Lenc, K., Mensch, A., Millican, K., Reynolds, M., Ring, R., Rutherford, E., Cabi, S., Han, T., Gong, Z., Samangooei, S., Monteiro, M., Menick, J. L., Borgeaud, S., Brock, A., Nematzadeh, A., Sharifzadeh, S., Binkowski, M., Barreira, R., Vinyals, O., Zisserman, A., and Simonyan, K. Flamingo: a Visual Language Model for Few-Shot Learning. In Koyejo, S., Mohamed, S., Agarwal, A., Belgrave, D., Cho, K., and Oh, A. (eds.), *Advances in Neural Information Processing Systems 35: Annual Conference on Neural Information Processing Systems 2022, NeurIPS 2022, New Orleans, LA, USA, November 28 - December 9, 2022*, 2022. URL `http://papers.nips.cc/paper_files/paper/2022/hash/960a172bc7fbf0177ccccbb411a7d800-Abstract-Conference.html`.

Azar, M. G., Rowland, M., Piot, B., Guo, D., Calandriello, D., Valko, M., and Munos, R. A General Theoretical Paradigm to Understand Learning from Human Preferences. *arXiv preprint arXiv:2310.12036*, 2023.

Bellemare, M. G., Naddaf, Y., Veness, J., and Bowling, M. The Arcade Learning Environment: An Evaluation Platform for General Agents. *Journal of Artificial Intelligence Research*, 47:253–279, 2013.

Beltagy, I., Peters, M. E., and Cohan, A. Longformer: The Long-Document Transformer. *arXiv preprint arXiv:2004.05150*, 2020.

Black, S., Leo, G., Wang, P., Leahy, C., and Biderman, S. GPT-Neo: Large Scale Autoregressive Language Modeling with Mesh-Tensorflow, March 2021.

Brockman, G., Cheung, V., Pettersson, L., Schneider, J., Schulman, J., Tang, J., and Zaremba, W. OpenAI Gym. *arXiv preprint arXiv:1606.01540*, 2016.

Brohan, A., Brown, N., Carbajal, J., Chebotar, Y., Chen, X., Choromanski, K., Ding, T., Driess, D., Dubey, A., Finn, C., Florence, P., Fu, C., Arenas, M. G., Gopalakrishnan, K., Han, K., Hausman, K., Herzog, A., Hsu, J., Ichter, B., Irpan, A., Joshi, N. J., Julian, R., Kalashnikov, D., Kuang, Y., Leal, I., Lee, L., Lee, T. E., Levine, S., Lu, Y., Michalewski, H., Mordatch, I., Pertsch, K., Rao, K., Reymann, K., Ryoo, M. S., Salazar, G., Sanketi, P., Sermanet, P., Singh, J., Singh, A., Soricut, R., Tran, H. T., Vanhoucke, V., Vuong, Q., Wahid, A., Welker, S., Wohlhart, P., Wu, J., Xia, F., Xiao, T., Xu, P., Xu, S., Yu, T., and Zitkovich, B. RT-2: Vision-Language-Action Models Transfer Web Knowledge to Robotic Control. *arXiv preprint arXiv:2307.15818*, 2023a.

Brohan, A., Brown, N., Carbajal, J., Chebotar, Y., Dabis, J., Finn, C., Gopalakrishnan, K., Hausman, K., Herzog, A., Hsu, J., Ibarz, J., Ichter, B., Irpan, A., Jackson, T., Jesmonth, S., Joshi, N. J., Julian, R., Kalashnikov, D., Kuang, Y., Leal, I., Lee, K., Levine, S., Lu, Y., Malla, U., Manjunath, D., Mordatch, I., Nachum, O., Parada, C., Peralta, J., Perez, E., Pertsch, K., Quiambao, J., Rao, K., Ryoo, M. S., Salazar, G., Sanketi, P. R., Sayed, K., Singh, J., Sontakke, S., Stone, A., Tan, C., Tran, H. T., Vanhoucke, V., Vega, S., Vuong, Q., Xia, F., Xiao, T., Xu, P., Xu, S., Yu, T., and Zitkovich, B. RT-1: Robotics Transformer for Real-World Control at Scale. In Bekris, K. E., Hauser, K., Herbert, S. L., and Yu, J. (eds.), *Robotics: Science and Systems XIX, Daegu, Republic of Korea, July 10-14, 2023*, 2023b. doi: 10.15607/RSS.2023.XIX.025. URL `https://doi.org/10.15607/RSS.2023.XIX.025`.

Brown, T. B., Mann, B., Ryder, N., Subbiah, M., Kaplan, J., Dhariwal, P., Neelakantan, A., Shyam, P., Sastry, G., Askell, A., Agarwal, S., Herbert-Voss, A., Krueger, G., Henighan, T., Child, R., Ramesh, A., Ziegler, D. M., Wu, J., Winter, C., Hesse, C., Chen, M., Sigler, E., Litwin, M., Gray, S., Chess, B., Clark, J., Berner, C., McCandlish, S., Radford, A., Sutskever, I., and Amodei, D. Language Models are Few-Shot Learners. In Larochelle, H., Ranzato, M., Hadsell, R., Balcan, M., and Lin, H. (eds.), *Advances in Neural Information Processing Systems 33: Annual Conference* *on Neural Information Processing Systems 2020, NeurIPS 2020, December 6-12, 2020, virtual*, 2020. URL `https://proceedings.neurips.cc/paper/2020/hash/1457c0d6bfcb4967418bfb8ac142f64a-Abstract.html`.

Chebotar, Y., Vuong, Q., Hausman, K., Xia, F., Lu, Y., Irpan, A., Kumar, A., Yu, T., Herzog, A., Pertsch, K., Gopalakrishnan, K., Ibarz, J., Nachum, O., Sontakke, S. A., Salazar, G., Tran, H. T., Peralta, J., Tan, C., Manjunath, D., Singh, J., Zitkovich, B., Jackson, T., Rao, K., Finn, C., and Levine, S. Q-Transformer: Scalable Offline Reinforcement Learning via Autoregressive Q-Functions. In Tan, J., Toussaint, M., and Darvish, K. (eds.), *Conference on Robot Learning, CoRL 2023, 6-9 November 2023, Atlanta, GA, USA*, volume 229 of *Proceedings of Machine Learning Research*, pp. 3909–3928. PMLR, 2023. URL `https://proceedings.mlr.press/v229/chebotar23a.html`.

Chen, L., Lu, K., Rajeswaran, A., Lee, K., Grover, A., Laskin, M., Abbeel, P., Srinivas, A., and Mordatch, I. Decision Transformer: Reinforcement Learning via Sequence Modeling. In Ranzato, M., Beygelzimer, A., Dauphin, Y. N., Liang, P., and Vaughan, J. W. (eds.), *Advances in Neural Information Processing Systems 34: Annual Conference on Neural Information Processing Systems 2021, NeurIPS 2021, December 6-14, 2021, virtual*, pp. 15084–15097, 2021. URL `https://proceedings.neurips.cc/paper/2021/hash/7f489f642a0ddb10272b5c31057f0663-Abstract.html`.

Chen, X., Wang, X., Changpinyo, S., Piergiovanni, A. J., Padlewski, P., Salz, D., Goodman, S., Grycner, A., Mustafa, B., Beyer, L., Kolesnikov, A., Puigcerver, J., Ding, N., Rong, K., Akbari, H., Mishra, G., Xue, L., Thapliyal, A. V., Bradbury, J., and Kuo, W. PaLI: A Jointly-Scaled Multilingual Language-Image Model. In *The Eleventh International Conference on Learning Representations, ICLR 2023, Kigali, Rwanda, May 1-5, 2023*. OpenReview.net, 2023. URL `https://openreview.net/pdf?id=mWVoBz4W0u`.

Chevalier-Boisvert, M., Bahdanau, D., Lahlou, S., Willems, L., Saharia, C., Nguyen, T. H., and Bengio, Y. BabyAI: A Platform to Study the Sample Efficiency of Grounded Language Learning. In *7th International Conference on Learning Representations, ICLR 2019, New Orleans, LA, USA, May 6-9, 2019*. OpenReview.net, 2019. URL `https://openreview.net/forum?id=rJeXCo0cYX`.

Chevalier-Boisvert, M., Dai, B., Towers, M., de Lazcano, R., Willems, L., Lahlou, S., Pal, S., Castro, P. S., and Terry, J. Minigrid & Miniworld: Modular & Customizable Reinforcement Learning Environments for Goal-Oriented Tasks. *arXiv preprint arXiv:2306.13831*, 2023.

Dosovitskiy, A., Beyer, L., Kolesnikov, A., Weissenborn, D., Zhai, X., Unterthiner, T., Dehghani, M., Minderer, M., Heigold, G., Gelly, S., Uszkoreit, J., and Houlsby, N. An Image is Worth 16x16 Words: Transformers for Image Recognition at Scale. In *9th International Conference on Learning Representations, ICLR 2021, Virtual Event, Austria, May 3-7, 2021*. OpenReview.net, 2021.

Driess, D., Xia, F., Sajjadi, M. S., Lynch, C., Chowdhery, A., Ichter, B., Wahid, A., Tompson, J., Vuong, Q., Yu, T., et al. PaLM-E: An Embodied Multimodal Language Model. *arXiv preprint arXiv:2303.03378*, 2023.

Espeholt, L., Soyer, H., Munos, R., Simonyan, K., Mnih, V., Ward, T., Doron, Y., Firoiu, V., Harley, T., Dunning, I., Legg, S., and Kavukcuoglu, K. IMPALA: Scalable Distributed Deep-RL with Importance Weighted Actor-Learner Architectures. In Dy, J. G. and Krause, A. (eds.), *Proceedings of the 35th International Conference on Machine Learning, ICML 2018, Stockholmsmässan, Stockholm, Sweden, July 10-15, 2018*, volume 80 of *Proceedings of Machine Learning Research*, pp. 1406–1415. PMLR, 2018. URL `http://proceedings.mlr.press/v80/espeholt18a.html`.

Foundation, W. Wikimedia Downloads. URL `https://dumps.wikimedia.org`.

Gugger, S., Debut, L., Wolf, T., Schmid, P., Mueller, Z., Mangrulkar, S., Sun, M., and Bossan, B. Accelerate: Training and Inference at Scale Made Simple, Efficient and Adaptable. `https://github.com/huggingface/accelerate`, 2022.

Janner, M., Li, Q., and Levine, S. Offline Reinforcement Learning as One Big Sequence Modeling Problem. In Ranzato, M., Beygelzimer, A., Dauphin, Y. N., Liang, P., and Vaughan, J. W. (eds.), *Advances in Neural Information Processing Systems 34: Annual Conference on Neural Information Processing Systems 2021, NeurIPS 2021, December 6-14, 2021, virtual*, pp. 1273–1286, 2021. URL https://proceedings.neurips.cc/paper/2021/hash/099fe6b0b444c23836c4a5d07346082b-Abstract.html.

Jiang, Y., Gupta, A., Zhang, Z., Wang, G., Dou, Y., Chen, Y., Fei-Fei, L., Anandkumar, A., Zhu, Y., and Fan, L. VIMA: General Robot Manipulation with Multimodal Prompts. *arXiv preprint arXiv:2210.03094*, 2022.

Kapturowski, S., Ostrovski, G., Quan, J., Munos, R., and Dabney, W. Recurrent Experience Replay in Distributed Reinforcement Learning. In *7th International Conference on Learning Representations, ICLR 2019, New Orleans, LA, USA, May 6-9, 2019*. OpenReview.net, 2019. URL https://openreview.net/forum?id=r1lyTjAqYX.

Laurençon, H., Saulnier, L., Tronchon, L., Bekman, S., Singh, A., Lozhkov, A., Wang, T., Karamcheti, S., Rush, A. M., Kiela, D., Cord, M., and Sanh, V. OBELISC: An Open Web-Scale Filtered Dataset of Interleaved Image-Text Documents. *arXiv preprint arXiv:2306.16527*, 2023a.

Laurençon, H., Saulnier, L., Wang, T., Akiki, C., del Moral, A. V., Scao, T. L., Werra, L. V., Mou, C., Ponferrada, E. G., Nguyen, H., Frohberg, J., Šaško, M., Lhoest, Q., McMillan-Major, A., Dupont, G., Biderman, S., Rogers, A., allal, L. B., Toni, F. D., Pistilli, G., Nguyen, O., Nikpoor, S., Masoud, M., Colombo, P., de la Rosa, J., Villegas, P., Thrush, T., Longpre, S., Nagel, S., Weber, L., Muñoz, M., Zhu, J., Strien, D. V., Alyafeai, Z., Almubarak, K., Vu, M. C., Gonzalez-Dios, I., Soroa, A., Lo, K., Dey, M., Suarez, P. O., Gokaslan, A., Bose, S., Adelani, D., Phan, L., Tran, H., Yu, I., Pai, S., Chim, J., Lepercq, V., Ilic, S., Mitchell, M., Luccioni, S. A., and Jernite, Y. The BigScience ROOTS Corpus: A 1.6TB Composite Multilingual Dataset. *arXiv preprint arXiv:2303.03915*, 2023b.

Lee, K.-H., Nachum, O., Yang, M. S., Lee, L., Freeman, D., Guadarrama, S., Fischer, I., Xu, W., Jang, E., Michalewski, H., and Mordatch, I. Multi-Game Decision Transformers. In Koyejo, S., Mohamed, S., Agarwal, A., Belgrave, D., Cho, K., and Oh, A. (eds.), *Advances in Neural Information Processing Systems 35: Annual Conference on Neural Information Processing Systems 2022, NeurIPS 2022, New Orleans, LA, USA, November 28 - December 9, 2022*, volume 35, pp. 27921–27936. Curran Associates, Inc., 2022. URL http://papers.nips.cc/paper_files/paper/2022/hash/b2cac94f82928a85055987d9fd44753f-Abstract-Conference.html.

Li, W., Luo, H., Lin, Z., Zhang, C., Lu, Z., and Ye, D. A Survey on Transformers in Reinforcement Learning. *Transactions on Machine Learning Research*, 2023. ISSN 2835-8856. URL https://openreview.net/forum?id=r30yuDPvf2. Survey Certification.

Liu, H. and Abbeel, P. Emergent Agentic Transformer from Chain of Hindsight Experience. In Krause, A., Brunskill, E., Cho, K., Engelhardt, B., Sabato, S., and Scarlett, J. (eds.), *International Conference on Machine Learning, ICML 2023, 23-29 July 2023, Honolulu, Hawaii, USA*, volume 202 of *Proceedings of Machine Learning Research*, pp. 21362–21374. PMLR, 2023.

Marino, K., Rastegari, M., Farhadi, A., and Mottaghi, R. OK-VQA: A Visual Question Answering Benchmark Requiring External Knowledge. In *IEEE Conference on Computer Vision and Pattern Recognition, CVPR 2019, Long Beach, CA, USA, June 16-20, 2019*, pp. 3195–3204. Computer Vision Foundation / IEEE, 2019.

Mnih, V., Kavukcuoglu, K., Silver, D., Rusu, A. A., Veness, J., Bellemare, M. G., Graves, A., Riedmiller, M., Fidjeland, A. K., Ostrovski, G., et al. Human-Level Control Through Deep Reinforcement Learning. *Nature*, 518(7540):529–533, 2015.

Moi, A. and Patry, N. HuggingFace's Tokenizers, April 2023.

Ortiz Suárez, P. J., Romary, L., and Sagot, B. A Monolingual Approach to Contextualized Word Embeddings for Mid-Resource Languages. In Jurafsky, D., Chai, J., Schluter, N., and Tetreault, J. (eds.), *Proceedings of the 58th Annual Meeting of the Association for Computational Linguistics*, pp. 1703–1714, Online, July 2020. Association for Computational Linguistics. doi: 10.18653/v1/2020.acl-main.156. URL https://aclanthology.org/2020.acl-main.156.

Ouyang, L., Wu, J., Jiang, X., Almeida, D., Wainwright, C. L., Mishkin, P., Zhang, C., Agarwal, S., Slama, K., Ray, A., Schulman, J., Hilton, J., Kelton, F., Miller, L., Simens, M., Askell, A., Welinder, P., Christiano, P. F., Leike, J., and Lowe, R. Training Language Models to Follow Instructions with Human Feedback. In Koyejo, S., Mohamed, S., Agarwal, A., Belgrave, D., Cho, K., and Oh, A. (eds.), *Advances in Neural Information Processing Systems 35: Annual Conference on Neural Information Processing Systems 2022, NeurIPS 2022, New Orleans, LA, USA, November 28 - December 9, 2022*, 2022. URL `http://papers.nips.cc/paper_files/paper/2022/hash/b1efde53be364a73914f58805a001731-Abstract-Conference.html`.

Parisotto, E., Ba, L. J., and Salakhutdinov, R. Actor-Mimic: Deep Multitask and Transfer Reinforcement Learning. In Bengio, Y. and LeCun, Y. (eds.), *4th International Conference on Learning Representations, ICLR 2016, San Juan, Puerto Rico, May 2-4, 2016, Conference Track Proceedings*, 2016. URL `http://arxiv.org/abs/1511.06342`.

Petrenko, A., Huang, Z., Kumar, T., Sukhatme, G. S., and Koltun, V. Sample Factory: Egocentric 3D Control from Pixels at 100000 FPS with Asynchronous Reinforcement Learning. In *Proceedings of the 37th International Conference on Machine Learning, ICML 2020, 13-18 July 2020, Virtual Event*, volume 119 of *Proceedings of Machine Learning Research*, pp. 7652–7662. PMLR, 2020. URL `http://proceedings.mlr.press/v119/petrenko20a.html`.

Radford, A., Wu, J., Child, R., Luan, D., Amodei, D., Sutskever, I., et al. Language Models are Unsupervised Multitask Learners. *OpenAI blog*, 1(8):9, 2019.

Rafailov, R., Sharma, A., Mitchell, E., Manning, C. D., Ermon, S., and Finn, C. Direct Preference Optimization: Your Language Model is Secretly a Reward Model. In Oh, A., Naumann, T., Globerson, A., Saenko, K., Hardt, M., and Levine, S. (eds.), *Advances in Neural Information Processing Systems 36: Annual Conference on Neural Information Processing Systems 2023, NeurIPS 2023, New Orleans, LA, USA, December 10 - 16, 2023*, 2023. URL `http://papers.nips.cc/paper_files/paper/2023/hash/a85b405ed65c6477a4fe8302b5e06ce7-Abstract-Conference.html`.

Raffel, C., Shazeer, N., Roberts, A., Lee, K., Narang, S., Matena, M., Zhou, Y., Li, W., and Liu, P. J. Exploring the Limits of Transfer Learning with a Unified Text-to-Text Transformer. *Journal of Machine Learning Research*, 21(140):1–67, 2020. ISSN 1533-7928. URL `http://jmlr.org/papers/v21/20-074.html`.

Reed, S., Zolna, K., Parisotto, E., Colmenarejo, S. G., Novikov, A., Barth-maron, G., Giménez, M., Sulsky, Y., Kay, J., Springenberg, J. T., Eccles, T., Bruce, J., Razavi, A., Edwards, A., Heess, N., Chen, Y., Hadsell, R., Vinyals, O., Bordbar, M., and de Freitas, N. A Generalist Agent. *Transactions on Machine Learning Research*, 2022. ISSN 2835-8856. Featured Certification, Outstanding Certification.

Rusu, A. A., Colmenarejo, S. G., Gülçehre, Ç., Desjardins, G., Kirkpatrick, J., Pascanu, R., Mnih, V., Kavukcuoglu, K., and Hadsell, R. Policy Distillation. In Bengio, Y. and LeCun, Y. (eds.), *4th International Conference on Learning Representations, ICLR 2016, San Juan, Puerto Rico, May 2-4, 2016, Conference Track Proceedings*, 2016. URL `http://arxiv.org/abs/1511.06295`.

Schulman, J., Wolski, F., Dhariwal, P., Radford, A., and Klimov, O. Proximal Policy Optimization Algorithms. *arXiv preprint arXiv:1707.06347*, 2017.

Sennrich, R., Haddow, B., and Birch, A. Neural Machine Translation of Rare Words with Subword Units. In *Proceedings of the 54th Annual Meeting of the Association for Computational Linguistics (Volume 1: Long Papers)*, pp. 1715–1725, 2016.

Sharma, P., Ding, N., Goodman, S., and Soricut, R. Conceptual Captions: A Cleaned, Hypernymed, Image Alt-text Dataset For Automatic Image Captioning. In Gurevych, I. and Miyao, Y. (eds.), *Proceedings of the 56th Annual Meeting of the Association for Computational Linguistics (Volume 1: Long Papers)*, pp. 2556–2565, Melbourne, Australia, July 2018. Association for Computational Linguistics.

Song, H. F., Abdolmaleki, A., Springenberg, J. T., Clark, A., Soyer, H., Rae, J. W., Noury, S., Ahuja, A., Liu, S., Tirumala, D., Heess, N., Belov, D., Riedmiller, M. A., and Botvinick, M. M. V-MPO:

On-Policy Maximum a Posteriori Policy Optimization for Discrete and Continuous Control. In *8th International Conference on Learning Representations, ICLR 2020, Addis Ababa, Ethiopia, April 26-30, 2020*. OpenReview.net, 2020. URL `https://openreview.net/forum?id=SylOlp4FvH`.

Tassa, Y., Doron, Y., Muldal, A., Erez, T., Li, Y., de Las Casas, D., Budden, D., Abdolmaleki, A., Merel, J., Lefrancq, A., Lillicrap, T. P., and Riedmiller, M. A. DeepMind Control Suite. *arXiv preprint arXiv:1801.00690*, 2018.

Teh, Y. W., Bapst, V., Czarnecki, W. M., Quan, J., Kirkpatrick, J., Hadsell, R., Heess, N., and Pascanu, R. Distral: Robust multitask reinforcement learning. In Guyon, I., von Luxburg, U., Bengio, S., Wallach, H. M., Fergus, R., Vishwanathan, S. V. N., and Garnett, R. (eds.), *Advances in Neural Information Processing Systems 30: Annual Conference on Neural Information Processing Systems 2017, December 4-9, 2017, Long Beach, CA, USA*, pp. 4496–4506, 2017. URL `https://proceedings.neurips.cc/paper/2017/hash/0abdc563a06105aee3c6136871c9f4d1-Abstract.html`.

Todorov, E., Erez, T., and Tassa, Y. MuJoCo: A physics engine for model-based control. In *2012 IEEE/RSJ International Conference on Intelligent Robots and Systems, IROS 2012, Vilamoura, Algarve, Portugal, October 7-12, 2012*, pp. 5026–5033. IEEE, 2012. doi: 10.1109/IROS.2012.6386109. URL `https://doi.org/10.1109/IROS.2012.6386109`.

Vaswani, A., Shazeer, N., Parmar, N., Uszkoreit, J., Jones, L., Gomez, A. N., Kaiser, L., and Polosukhin, I. Attention is All you Need. In Guyon, I., von Luxburg, U., Bengio, S., Wallach, H. M., Fergus, R., Vishwanathan, S. V. N., and Garnett, R. (eds.), *Advances in Neural Information Processing Systems 30: Annual Conference on Neural Information Processing Systems 2017, December 4-9, 2017, Long Beach, CA, USA*, pp. 5998–6008, 2017. URL `https://proceedings.neurips.cc/paper/2017/hash/3f5ee243547dee91fbd053c1c4a845aa-Abstract.html`.

Wolf, T., Debut, L., Sanh, V., Chaumond, J., Delangue, C., Moi, A., Cistac, P., Rault, T., Louf, R., Funtowicz, M., Davison, J., Shleifer, S., von Platen, P., Ma, C., Jernite, Y., Plu, J., Xu, C., Scao, T. L., Gugger, S., Drame, M., Lhoest, Q., and Rush, A. M. Transformers: State-of-the-Art Natural Language Processing. In *Proceedings of the 2020 Conference on Empirical Methods in Natural Language Processing: System Demonstrations*, pp. 38–45. Association for Computational Linguistics, October 2020. URL `https://www.aclweb.org/anthology/2020.emnlp-demos.6`.

Yang, R., Xu, H., Wu, Y., and Wang, X. Multi-Task Reinforcement Learning with Soft Modularization. In Larochelle, H., Ranzato, M., Hadsell, R., Balcan, M., and Lin, H. (eds.), *Advances in Neural Information Processing Systems 33: Annual Conference on Neural Information Processing Systems 2020, NeurIPS 2020, December 6-12, 2020, virtual*, 2020. URL `https://proceedings.neurips.cc/paper/2020/hash/32cfdce9631d8c7906e8e9d6e68b514b-Abstract.html`.

Yu, T., Quillen, D., He, Z., Julian, R., Hausman, K., Finn, C., and Levine, S. Meta-World: A Benchmark and Evaluation for Multi-Task and Meta Reinforcement Learning. In Kaelbling, L. P., Kragic, D., and Sugiura, K. (eds.), *3rd Annual Conference on Robot Learning, CoRL 2019, Osaka, Japan, October 30 - November 1, 2019, Proceedings*, volume 100 of *Proceedings of Machine Learning Research*, pp. 1094–1100. PMLR, 2019. URL `http://proceedings.mlr.press/v100/yu20a.html`.

Zeiler, M. D., Krishnan, D., Taylor, G. W., and Fergus, R. Deconvolutional Networks. In *The Twenty-Third IEEE Conference on Computer Vision and Pattern Recognition, CVPR 2010, San Francisco, CA, USA, 13-18 June 2010*, pp. 2528–2535. IEEE Computer Society, 2010. URL `https://doi.org/10.1109/CVPR.2010.5539957`.

Zheng, Q., Zhang, A., and Grover, A. Online Decision Transformer. *arXiv preprint arXiv:2202.05607*, 2022.

A Full results

This appendix contains a detailed view of the results of the trained JAT agent. The score of the random agent for Atari games is sourced from (Mnih et al., 2015). In other domains, this score is approximated by averaging the returns from 1,000 episodes, where the agent selects actions uniformly across its action space. The expert scores represent the average return in the dataset for the task. Meanwhile, the raw score is the average return achieved by the trained agent, based on 100 evaluation episodes. Both these scores, along with the trained agent, are accessible as open-source[3]. The normalized score is derived by comparing the agent's return to the expert's, calculated using the formula: $\frac{\text{score}-\text{random\_score}}{\text{expert\_score}-\text{random\_score}}$. It's important to note that in instances where the *expert*, inaccurately named, does not fully master the task and thus scores similarly or lower than the random agent, the normalized score must be interpreted cautiously. Specifically, if this score falls below that of the random agent, as in the case of Bowling, normalization is not applied. The results for Atari are presented in Table 1 and Figure 7, for BabyAI in Table 2 and Figure 8, for Meta-World in Table 3 and Figure 9, and for MuJoCo in Table 4 and Figure 10.

[3] `https://huggingface.co/jat-project/jat`

Table 1: Comparison of performance scores across tasks on Atari 57. The table presents the episodic return (score) achieved by a random agent (from (Mnih et al., 2015)), scores of the expert agent (as averaged from the dataset), scores of the learned agent, and the expert normalized score calculated as $\frac{\text{score}-\text{random\_score}}{\text{expert\_score}-\text{random\_score}}$.

Task	Random agent	Expert	JAT (raw)	JAT (normalized)
Alien	227.8	16912.5 ± 7087.4	1474.9 ± 588.7	0.07 ± 0.04
Amidar	5.8	2164.7 ± 1229.5	104.9 ± 103.5	0.05 ± 0.05
Assault	222.4	15699.1 ± 9572.1	1650.1 ± 821.0	0.09 ± 0.05
Asterix	210.0	3699.6 ± 2421.3	800.0 ± 584.9	0.17 ± 0.17
Asteroids	719.0	177011.1 ± 35334.2	1385.3 ± 507.5	0.00 ± 0.00
Atlantis	12850.0	320679.6 ± 418247.4	66980.0 ± 158449.7	0.18 ± 0.51
Bank Heist	14.2	1322.4 ± 60.8	948.3 ± 199.9	0.71 ± 0.15
Battle Zone	236.0	295592.6 ± 161961.0	17420.0 ± 6071.5	0.06 ± 0.02
Beam Rider	363.9	29589.3 ± 16133.0	797.3 ± 328.3	0.01 ± 0.01
Berzerk	123.7	57085.3 ± 13104.5	687.3 ± 331.9	0.01 ± 0.01
Bowling	23.1	20.4 ± 7.3	22.4 ± 5.6	N/A
Boxing	0.1	98.0 ± 3.8	90.1 ± 23.0	0.92 ± 0.24
Breakout	1.7	703.0 ± 203.6	8.8 ± 5.6	0.01 ± 0.01
Centipede	2090.9	11624.3 ± 4918.3	5589.9 ± 2567.3	0.37 ± 0.27
Chopper Command	811.0	90990.6 ± 270876.9	2417.0 ± 1489.9	0.02 ± 0.02
Crazy Climber	10780.5	179296.9 ± 39862.1	97639.0 ± 26184.7	0.52 ± 0.16
Defender	2874.5	351958.3 ± 40466.8	39323.5 ± 15203.0	0.10 ± 0.04
Demon Attack	152.1	92195.2 ± 26174.8	815.3 ± 989.7	0.01 ± 0.01
Double Dunk	-18.6	20.9 ± 3.6	14.4 ± 10.0	0.84 ± 0.25
Enduro	0.0	2292.2 ± 147.5	108.5 ± 42.7	0.05 ± 0.02
Fishing Derby	-91.7	7.2 ± 25.1	-30.4 ± 24.4	0.62 ± 0.25
Freeway	0.0	33.9 ± 0.3	27.5 ± 1.6	0.81 ± 0.05
Frostbite	65.2	13196.1 ± 4341.0	2769.6 ± 1445.6	0.21 ± 0.11
Gopher	257.6	81676.2 ± 46329.5	5340.6 ± 2547.1	0.06 ± 0.03
Gravitar	173.0	3986.6 ± 1729.0	1269.5 ± 903.0	0.29 ± 0.24
H.E.R.O.	1027.0	44677.4 ± 1754.4	11709.6 ± 3233.5	0.24 ± 0.07
Ice Hockey	-11.2	25.2 ± 5.8	7.5 ± 5.6	0.51 ± 0.15
James Bond	29.0	27786.9 ± 33819.2	327.5 ± 123.2	0.01 ± 0.00
Kangaroo	52.0	574.0 ± 636.9	378.0 ± 344.0	0.62 ± 0.66
Krull	1598.0	11439.8 ± 1218.3	10720.5 ± 1284.1	0.93 ± 0.13
Kung-Fu Master	258.5	32392.8 ± 10006.6	288.0 ± 255.1	0.00 ± 0.01
Montezuma's Revenge	0.0	393.5 ± 50.4	0.0 ± 0.0	0.00 ± 0.00
Ms. Pacman	307.3	6896.1 ± 2032.0	1573.1 ± 484.0	0.19 ± 0.07
Name This Game	2292.3	22991.2 ± 2473.1	7523.3 ± 2471.4	0.25 ± 0.12
Phoenix	761.5	424583.2 ± 97649.2	2197.9 ± 1795.4	0.00 ± 0.00
PitFall	-229.4	-1.4 ± 4.5	-6.7 ± 19.0	0.98 ± 0.08
Pong	-20.7	21.0 ± 0.2	13.7 ± 13.3	0.82 ± 0.32
Private Eye	24.9	100.0 ± 0.0	44.0 ± 49.6	0.25 ± 0.66
Q*Bert	163.9	42971.4 ± 85070.7	1951.5 ± 2577.2	0.04 ± 0.06
River Raid	1338.5	14800.9 ± 7924.6	3758.5 ± 1536.7	0.18 ± 0.11
Road Runner	11.5	77942.8 ± 6088.6	6407.0 ± 4847.4	0.08 ± 0.06
Robotank	2.2	80.5 ± 13.3	11.3 ± 5.5	0.12 ± 0.07
Seaquest	68.4	2597.3 ± 386.1	804.0 ± 403.3	0.29 ± 0.16
Skiing	-17098.0	-10738.1 ± 111.1	-16231.5 ± 6060.5	0.14 ± 0.95
Solaris	1236.3	1353.7 ± 517.0	1286.6 ± 446.7	0.43 ± 3.81
Space Invaders	148.0	29425.3 ± 23623.9	325.4 ± 163.4	0.01 ± 0.01
Star Gunner	664.0	360588.6 ± 49207.7	4379.0 ± 3027.2	0.01 ± 0.01
Surround	-10.0	9.4 ± 0.8	2.7 ± 4.7	0.65 ± 0.24
Tennis	-23.8	11.1 ± 7.6	-13.5 ± 3.8	0.30 ± 0.11
Time Pilot	3568.0	69583.3 ± 29838.7	13028.0 ± 5222.6	0.14 ± 0.08
Tutankham	11.4	291.2 ± 30.4	85.7 ± 61.8	0.27 ± 0.22
Up and Down	533.4	429418.3 ± 7187.4	17768.7 ± 10322.0	0.04 ± 0.02
Venture	0.0	0.0 ± 0.0	0.0 ± 0.0	N/A
Video Pinball	0.0	441507.9 ± 283264.6	11917.4 ± 8204.3	0.03 ± 0.02
Wizard of Wor	563.5	49333.3 ± 16157.1	2544.0 ± 2902.4	0.04 ± 0.06
Yars Revenge	3092.9	270262.9 ± 161816.0	12532.7 ± 8062.8	0.04 ± 0.03
Zaxxon	32.5	73097.2 ± 14825.8	6902.0 ± 3206.1	0.09 ± 0.04

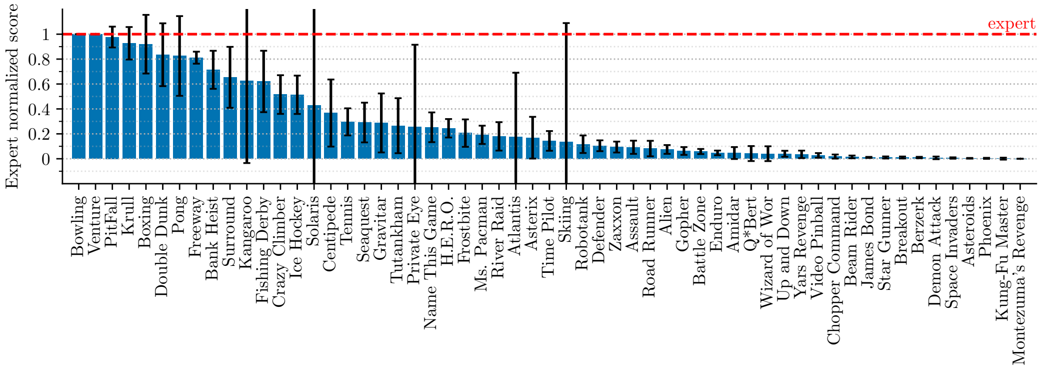

Figure 7: Expert normalized episodic return for the JAT agent on the Atari 57 benchmark.

Table 2: Comparison of performance scores across tasks on BabyAI. The table presents the episodic return (score) achieved by a random agent (averaged over 1,000 episodes), scores of the expert agent (as averaged from the dataset), scores of the learned agent, and the expert normalized score calculated as $\frac{\text{score}-\text{random\_score}}{\text{expert\_score}-\text{random\_score}}$.

Task	Random Agent	Expert	JAT (raw)	JAT (normalized)
Action Obj Door	0.37 ± 0.39	0.99 ± 0.01	0.94 ± 0.14	0.93 ± 0.23
Blocked Unlock Pickup	0.00 ± 0.02	0.95 ± 0.01	0.95 ± 0.01	1.00 ± 0.01
Boss Level	0.06 ± 0.21	0.94 ± 0.05	0.52 ± 0.43	0.53 ± 0.49
Boss Level No Unlock	0.06 ± 0.19	0.94 ± 0.05	0.48 ± 0.43	0.48 ± 0.48
Find Obj S5	0.08 ± 0.23	0.95 ± 0.04	0.95 ± 0.04	1.01 ± 0.05
Go To	0.13 ± 0.29	0.92 ± 0.07	0.83 ± 0.27	0.89 ± 0.34
Go To Door	0.45 ± 0.38	0.99 ± 0.00	0.99 ± 0.02	0.99 ± 0.04
Go To Imp Unlock	0.07 ± 0.22	0.83 ± 0.13	0.60 ± 0.41	0.70 ± 0.54
Go To Local	0.16 ± 0.30	0.93 ± 0.04	0.88 ± 0.14	0.94 ± 0.19
Go To Obj	0.13 ± 0.27	0.93 ± 0.03	0.93 ± 0.03	1.00 ± 0.04
Go To Obj Door	0.53 ± 0.39	0.99 ± 0.01	0.96 ± 0.10	0.94 ± 0.21
Go To Red Ball	0.17 ± 0.30	0.93 ± 0.04	0.92 ± 0.05	0.99 ± 0.07
Go To Red Ball Grey	0.12 ± 0.27	0.92 ± 0.05	0.91 ± 0.07	0.99 ± 0.08
Go To Red Ball No Dists	0.14 ± 0.28	0.93 ± 0.03	0.93 ± 0.03	1.00 ± 0.04
Go To Red Blue Ball	0.12 ± 0.27	0.92 ± 0.05	0.88 ± 0.11	0.95 ± 0.14
Go To Seq	0.08 ± 0.23	0.94 ± 0.05	0.72 ± 0.34	0.74 ± 0.40
Key Corridor	0.00 ± 0.00	0.91 ± 0.01	0.86 ± 0.16	0.94 ± 0.18
Mini Boss Level	0.07 ± 0.21	0.89 ± 0.10	0.61 ± 0.39	0.65 ± 0.47
Move Two Across S8N9	0.00 ± 0.00	0.96 ± 0.01	0.02 ± 0.13	0.02 ± 0.13
One Room S8	0.08 ± 0.21	0.92 ± 0.03	0.92 ± 0.04	1.00 ± 0.04
Open	0.10 ± 0.24	0.95 ± 0.05	0.94 ± 0.11	0.98 ± 0.13
Open Door	0.23 ± 0.34	0.99 ± 0.00	0.99 ± 0.00	1.00 ± 0.01
Open Doors Order N4	0.16 ± 0.30	0.99 ± 0.01	0.95 ± 0.17	0.95 ± 0.20
Open Red Door	0.08 ± 0.21	0.92 ± 0.03	0.91 ± 0.03	1.00 ± 0.04
Open Two Doors	0.08 ± 0.20	0.98 ± 0.00	0.98 ± 0.00	1.00 ± 0.00
Pickup	0.08 ± 0.22	0.92 ± 0.07	0.76 ± 0.32	0.82 ± 0.38
Pickup Above	0.02 ± 0.09	0.91 ± 0.07	0.90 ± 0.08	0.99 ± 0.09
Pickup Dist	0.10 ± 0.24	0.86 ± 0.21	0.90 ± 0.07	1.05 ± 0.09
Pickup Loc	0.08 ± 0.23	0.91 ± 0.04	0.86 ± 0.16	0.94 ± 0.19
Put Next S7N4	0.00 ± 0.03	0.96 ± 0.01	0.85 ± 0.22	0.88 ± 0.23
Put Next Local	0.00 ± 0.05	0.92 ± 0.03	0.63 ± 0.36	0.69 ± 0.40
Synth	0.11 ± 0.26	0.93 ± 0.06	0.77 ± 0.33	0.80 ± 0.40
Synth Loc	0.13 ± 0.29	0.94 ± 0.06	0.79 ± 0.33	0.81 ± 0.40
Synth Seq	0.07 ± 0.20	0.95 ± 0.04	0.52 ± 0.44	0.52 ± 0.50
Unblock Pickup	0.08 ± 0.22	0.91 ± 0.08	0.74 ± 0.32	0.79 ± 0.39
Unlock	0.03 ± 0.15	0.87 ± 0.10	0.52 ± 0.42	0.58 ± 0.50
Unlock Local	0.01 ± 0.09	0.98 ± 0.01	0.98 ± 0.01	1.00 ± 0.01
Unlock Pickup	0.00 ± 0.00	0.75 ± 0.04	0.76 ± 0.04	1.01 ± 0.05
Unlock To Unlock	0.00 ± 0.00	0.96 ± 0.00	0.80 ± 0.35	0.83 ± 0.37

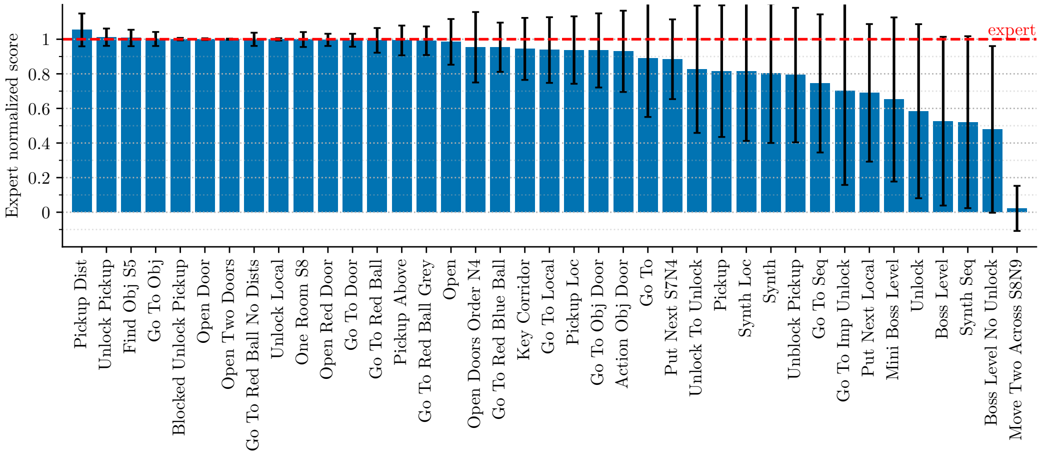

Figure 8: Expert normalized episodic return for the JAT agent on the BabyAI benchmark.

Table 3: Comparison of performance scores across tasks on Meta-World. The table presents the episodic return (score) achieved by a random agent (averaged over 1,000 episodes), scores of the expert agent (as averaged from the dataset), scores of the learned agent, and the expert normalized score calculated as $\frac{\text{score}-\text{random\_score}}{\text{expert\_score}-\text{random\_score}}$.

Task	Random agent	Expert	JAT (raw)	JAT (normalized)
Assembly	45.3 ± 4.1	246.0 ± 3.5	238.0 ± 34.6	0.96 ± 0.17
Basketball	2.8 ± 1.2	628.0 ± 2.0	1.6 ± 0.4	-0.00 ± 0.00
BinPicking	1.9 ± 0.4	425.6 ± 101.9	200.0 ± 222.1	0.47 ± 0.52
Box Close	76.4 ± 17.9	512.5 ± 107.8	462.6 ± 172.0	0.89 ± 0.39
Button Press	31.7 ± 5.2	643.1 ± 12.8	560.0 ± 182.6	0.86 ± 0.30
Button Press Topdown	29.0 ± 10.4	490.2 ± 27.2	266.2 ± 77.2	0.51 ± 0.17
Button Press Topdown Wall	29.0 ± 10.5	497.2 ± 31.4	275.8 ± 88.6	0.53 ± 0.19
Button Press Wall	9.0 ± 4.0	675.4 ± 15.0	638.3 ± 123.0	0.94 ± 0.18
Coffee Button	31.7 ± 6.4	731.1 ± 29.3	298.0 ± 285.6	0.38 ± 0.41
Coffee Pull	4.1 ± 0.4	259.9 ± 88.5	41.0 ± 69.8	0.14 ± 0.27
Coffee Push	4.2 ± 0.8	496.8 ± 118.2	153.1 ± 218.9	0.30 ± 0.44
Dial Turn	29.6 ± 16.7	793.6 ± 80.1	758.4 ± 120.4	0.95 ± 0.16
Disassemble	40.3 ± 7.5	42.8 ± 6.3	40.7 ± 9.9	0.17 ± 3.91
Door Close	5.3 ± 1.3	529.7 ± 27.2	524.3 ± 33.2	0.99 ± 0.06
Door Lock	112.3 ± 28.6	811.5 ± 34.1	696.3 ± 198.6	0.84 ± 0.28
Door Open	56.4 ± 11.2	581.9 ± 19.7	577.5 ± 53.7	0.99 ± 0.10
Door Unlock	94.2 ± 15.6	802.9 ± 17.1	768.3 ± 91.8	0.95 ± 0.13
Drawer Close	116.7 ± 253.1	867.9 ± 4.5	596.7 ± 223.4	0.64 ± 0.30
Drawer Open	126.8 ± 25.2	493.0 ± 2.5	485.9 ± 36.8	0.98 ± 0.10
Faucet Close	253.1 ± 22.9	753.9 ± 13.4	367.8 ± 91.1	0.23 ± 0.18
Faucet Open	244.1 ± 23.3	705.8 ± 7.1	566.1 ± 169.9	0.70 ± 0.37
Hammer	95.3 ± 9.0	693.2 ± 34.6	667.7 ± 89.4	0.96 ± 0.15
Hand Insert	2.8 ± 3.5	740.5 ± 36.7	688.1 ± 187.7	0.93 ± 0.25
Handle Press	80.4 ± 110.2	855.9 ± 72.7	735.0 ± 252.0	0.84 ± 0.32
Handle Press Side	57.0 ± 39.5	861.1 ± 20.0	64.5 ± 73.7	0.01 ± 0.09
Handle Pull	10.3 ± 13.5	669.4 ± 24.8	556.6 ± 161.7	0.83 ± 0.25
Handle Pull Side	2.1 ± 2.8	384.7 ± 102.9	195.1 ± 187.2	0.50 ± 0.49
Lever Pull	60.3 ± 15.8	612.0 ± 38.9	280.9 ± 234.8	0.40 ± 0.43
Peg Insert Side	1.7 ± 0.4	315.2 ± 140.1	254.3 ± 158.4	0.81 ± 0.51
Peg Unplug Side	4.7 ± 2.8	456.1 ± 81.7	80.6 ± 145.5	0.17 ± 0.32
Pick Out Of Hole	1.5 ± 0.2	219.6 ± 88.9	2.1 ± 0.1	0.00 ± 0.00
Pick Place	1.6 ± 1.0	419.1 ± 98.2	135.8 ± 200.1	0.32 ± 0.48
Pick Place Wall	0.0 ± 0.0	450.6 ± 64.1	43.7 ± 129.7	0.10 ± 0.29
Plate Slide	74.6 ± 13.8	527.0 ± 155.3	481.5 ± 190.2	0.90 ± 0.42
Plate Slide Back	33.5 ± 11.2	718.2 ± 87.4	196.9 ± 1.7	0.24 ± 0.00
Plate Slide Back Side	34.3 ± 11.5	729.6 ± 69.1	703.7 ± 117.3	0.96 ± 0.17
Plate Slide Side	22.6 ± 17.4	662.8 ± 102.8	122.6 ± 24.6	0.16 ± 0.04
Push	5.5 ± 2.4	750.6 ± 44.0	702.4 ± 157.6	0.94 ± 0.21
Push Back	1.2 ± 0.2	85.0 ± 107.1	82.2 ± 108.0	0.97 ± 1.29
Push Wall	6.1 ± 3.2	748.9 ± 10.6	158.8 ± 224.6	0.21 ± 0.30
Reach	149.7 ± 44.7	681.4 ± 133.7	332.2 ± 171.5	0.34 ± 0.32
Reach Wall	143.3 ± 36.6	746.1 ± 104.2	631.6 ± 224.0	0.81 ± 0.37
Shelf Place	0.0 ± 0.0	241.3 ± 24.6	92.1 ± 112.0	0.38 ± 0.46
Soccer	5.7 ± 4.6	375.2 ± 140.2	291.6 ± 161.8	0.77 ± 0.44
Stick Pull	2.6 ± 1.4	523.6 ± 18.9	480.1 ± 119.3	0.92 ± 0.23
Stick Push	2.8 ± 1.0	627.9 ± 10.2	303.2 ± 298.8	0.48 ± 0.48
Sweep	11.2 ± 7.3	494.8 ± 43.3	16.7 ± 18.7	0.01 ± 0.04
Sweep Into	12.5 ± 10.7	799.2 ± 19.1	793.3 ± 47.5	0.99 ± 0.06
Window Close	57.5 ± 7.1	591.3 ± 38.6	414.3 ± 207.4	0.67 ± 0.39
Window Open	43.4 ± 2.1	590.8 ± 57.1	577.3 ± 63.9	0.98 ± 0.12

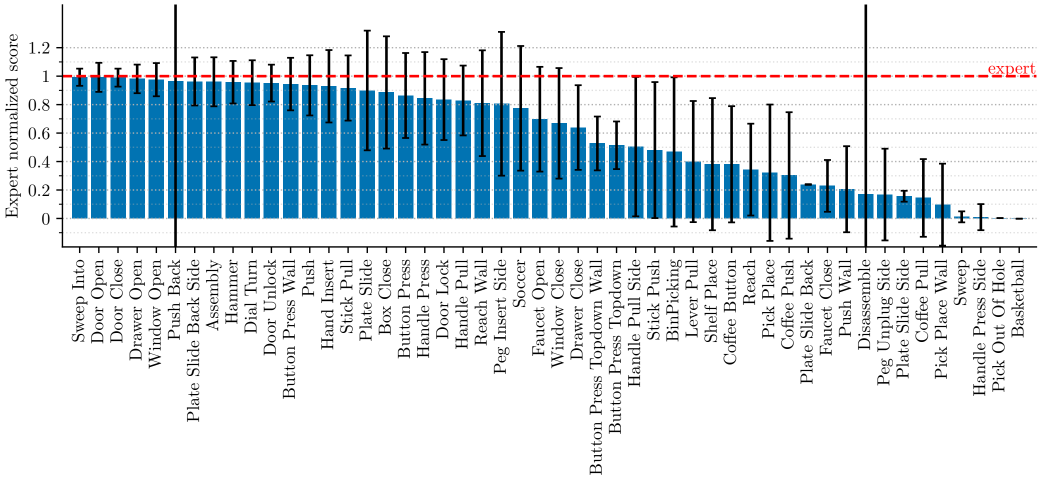

Figure 9: Expert normalized episodic return for the JAT agent on the Meta-World benchmark.

Table 4: Comparison of performance scores across tasks on MuJoCo. The table presents the episodic return (score) achieved by a random agent (averaged over 1,000 episodes), scores of the expert agent (as averaged from the dataset), scores of the learned agent, and the expert normalized score calculated as $\frac{\text{score}-\text{random\_score}}{\text{expert\_score}-\text{random\_score}}$.

TASK	RANDOM AGENT	EXPERT	JAT (RAW)	JAT (NORMALIZED)
ANT	-59.9 ± 99.6	5846.4 ± 942.6	5110.5 ± 1720.8	0.88 ± 0.29
INVERTED DOUBLE PENDULUM	57.5 ± 17.5	9338.7 ± 352.6	8663.7 ± 1259.4	0.93 ± 0.14
HALF CHEETAH	-285.0 ± 79.8	7437.8 ± 173.3	6595.9 ± 244.4	0.89 ± 0.03
HOPPER	18.4 ± 17.1	1858.7 ± 534.1	1409.0 ± 385.6	0.76 ± 0.21
HUMANOID	122.0 ± 35.3	6281.0 ± 1795.8	712.6 ± 120.6	0.10 ± 0.02
INVERTED PENDULUM	6.1 ± 3.5	475.4 ± 179.0	117.4 ± 22.0	0.24 ± 0.05
PUSHER	-149.7 ± 7.4	-25.2 ± 6.7	-25.0 ± 6.3	1.00 ± 0.05
REACHER	-43.0 ± 3.9	-5.7 ± 2.5	-5.9 ± 2.4	0.99 ± 0.06
HUMANOID STANDUP	33135.8 ± 2481.9	273574.2 ± 85253.3	116736.7 ± 22765.5	0.35 ± 0.09
SWIMMER	0.8 ± 10.7	92.2 ± 4.4	94.0 ± 4.1	1.02 ± 0.04
WALKER 2D	2.7 ± 6.1	4631.2 ± 1059.0	4381.3 ± 851.1	0.95 ± 0.18

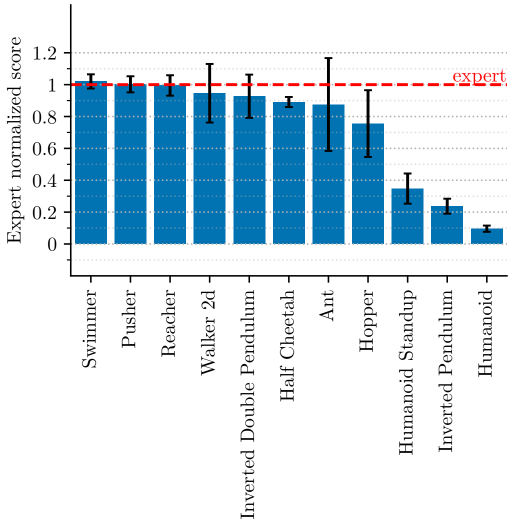

Figure 10: Expert normalized episodic return for the JAT agent on the MuJoCo benchmark.

B JAT Dataset In Depth

B.1 Sequential Decision-Making Datasets

For each decision-making environment, we collect a set of interactions using expert agents. Detailed scores are available in the Appendix A.

Atari We use the 57 games from the Arcade Learning Environment (Bellemare et al., 2013, ALE) as a benchmark in our research, amassing roughly 500,000 interactions per game. Episode lengths varied significantly depending on the specific game. For each game, we trained a dedicated agent for 2 billion steps using the asynchronous implementation of Proximal Policy Optimization (Schulman et al., 2017) from Sample Factory (Petrenko et al., 2020). The expert agents achieve above human performance on 43 tasks[4].

BabyAI BabyAI stands out in our study due to its unique characteristic of being partially observable and its dual-modality observations (Chevalier-Boisvert et al., 2019; Chevalier-Boisvert et al., 2023). Using the bot provided with the BabyAI paper (Chevalier-Boisvert et al., 2019), we gathered 100,000 episodes for 39 of its available settings. Each interaction consists of a text observation (mission), a discrete observation (7×7 symbolic representation of the agent's field of view), an action, and a reward.

Meta-World Meta-World's MT50 benchmark provides a set of 50 diverse and challenging robot manipulation tasks (Yu et al., 2019). Similar to the methodology used for Atari, we trained one agent per task using the asynchronous PPO (Schulman et al., 2017) implementation of (Petrenko et al., 2020). The trained agents solved most of the tasks, except for Assembly and Disassemble, where they failed to reach the expected performance. We limit the number of timesteps per episode to 100, which proved to be sufficient for solving the tasks. Without this limit, much of the subsequent dataset would consist of the stabilization phases of the agents after goal attainment, reducing its relevance. We then used the trained agents to generate 10,000 episodes per environment.

MuJoCo We included the MuJoCo locomotion benchmark suite (Todorov et al., 2012; Brockman et al., 2016) comprising 11 continuous control tasks into our study due to its diverse challenges in domain complexity and task difficulty, and its wide recognition in the research literature. Following our methodologies for Atari and Meta-World, we individually trained agents for each task using asynchronous PPO (Schulman et al., 2017) from Sample Factory (Petrenko et al., 2020). These agents successfully solved all tasks, achieving scores that meet or exceed the current highest standards. Subsequently, we employed these agents to generate 10,000 episodes per environment.

Each sample in this dataset is an episode. This episode consists of a list of observations, actions and rewards, the nature and size of which depend on the task. In Figure 11, we represent for each Atari game the average return of the episodes of the dataset normalized by the human score from (Mnih et al., 2015). Notably, for 43 games the average score is higher than the human score, and for 31 games the average score is more than twice the human score. It should be noted, however, that for 7 games (Bowling, Montezuma's Revenge, PitFall, Private Eye, Seaquest, Solaris and Venture) the average score is less than 10% of the human score.

We also plot the distribution of returns for each task, which provides a more detailed picture than a simple average. Figure 12 shows this distribution for Atari, Figure 13 for BabyAI, Figure 14 for Meta-World and Figure 15 for MuJoCo.

[4] The expert score is below the human score for Asterix, Bowling, Centipede, Fishing Derby, Kangaroo, Montezuma's Revenge, Ms. Pacman, Pitfall, Private Eye, River Raid, Seaquest, Skiing, Solaris, Venture

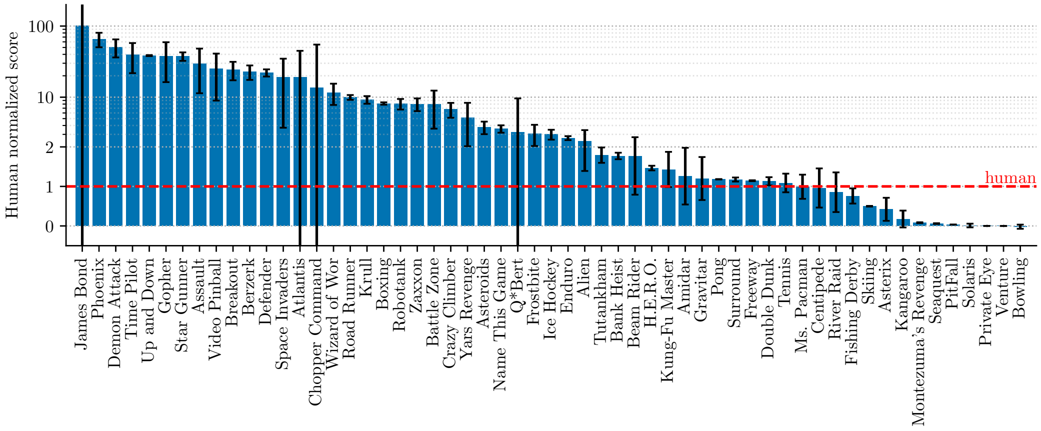

Figure 11: Human normalized dataset scores for Atari.

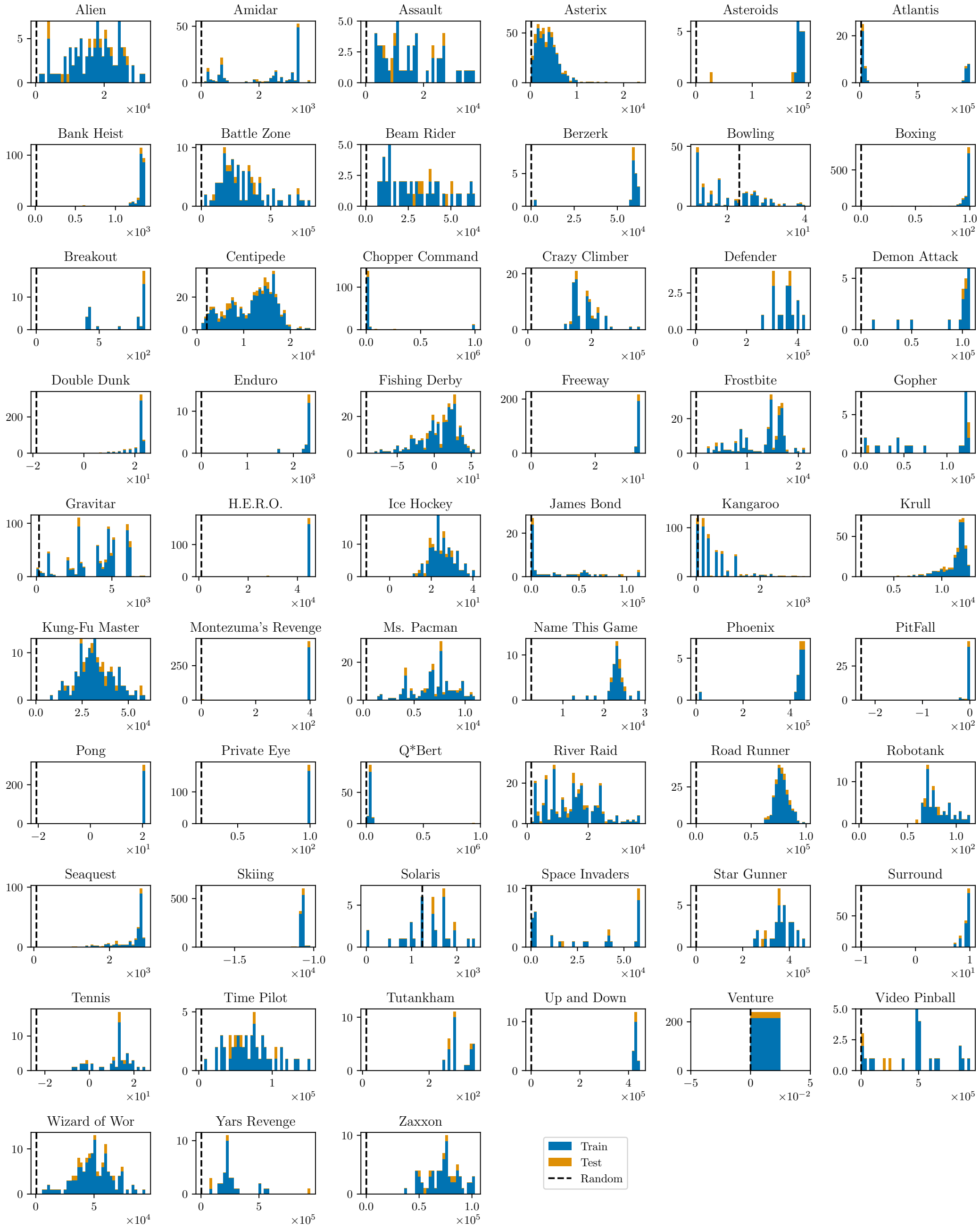

Figure 12: Atari dataset return distribution.

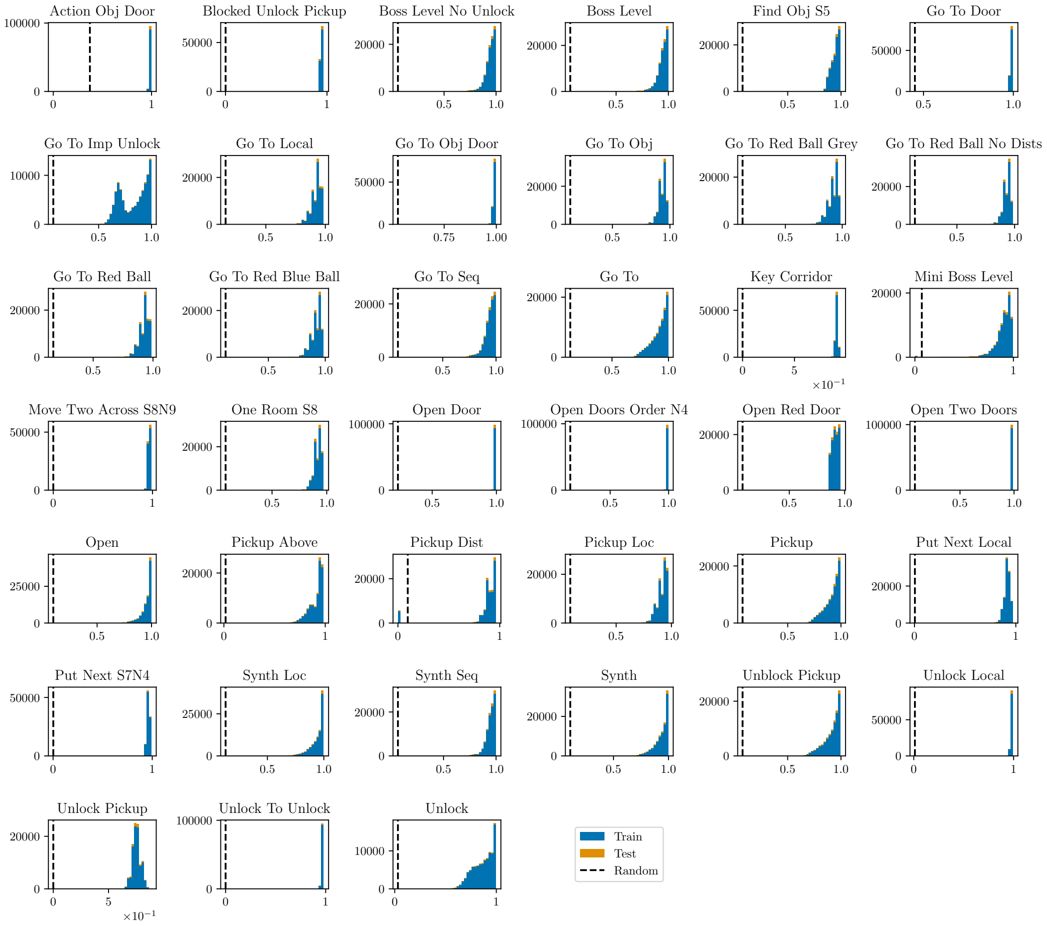

Figure 13: BabyAI dataset return distribution.

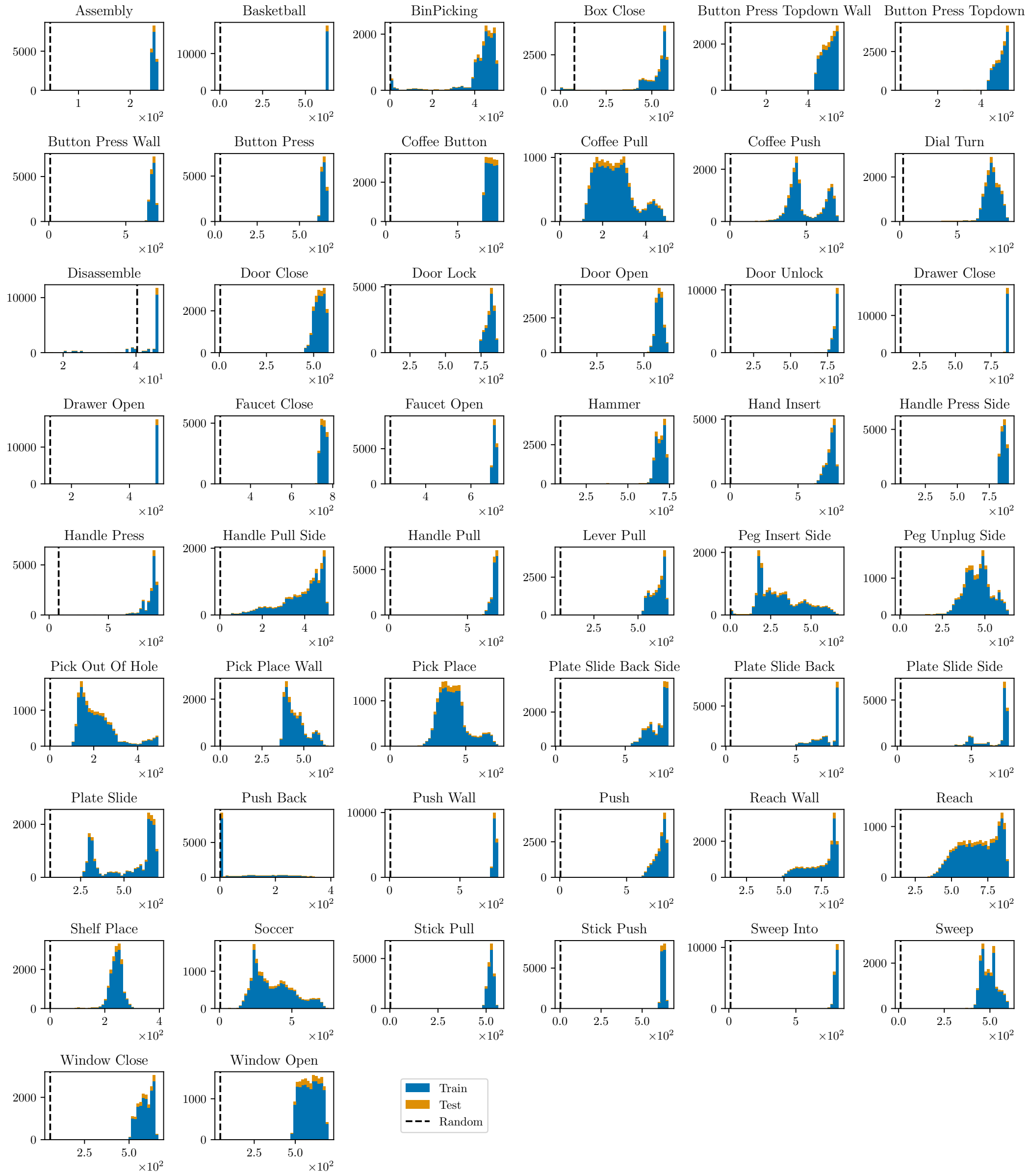

Figure 14: Meta-World dataset return distribution.

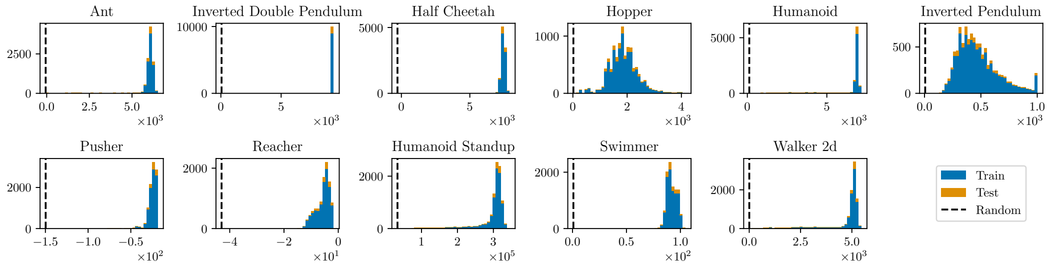

Figure 15: MuJoCo dataset return distribution.

B.1.1 Text-Centric Datasets

Oscar Common Crawl-based text documents have been widely used in the past to create datasets for Language Modeling (Radford et al., 2019; Brown et al., 2020; Raffel et al., 2020). We chose to leverage the unshuffled deduplicated English subset of the OSCAR[5] corpus (Ortiz Suárez et al., 2020) for our language modeling objective. As such crawled internet data needs to be cleaned before using it for training Language Models (e.g. deduplication, filtering out machine-generating content), we reused both the cleaning and deduplication pipeline from the ROOTS corpus (Laurençon et al., 2023b). The initial dataset was shuffled, split into a training (95%) and test (5%) set, and evenly split into 30 shards on which the cleaning and deduplication pipelines were applied to reduce the memory needs. Shards were then concatenated back together, leading to a final dataset of 245 million documents (compared to 304 million documents in the initial dataset).

Conceptual-Captions We include the Conceptual-Captions dataset (Sharma et al., 2018), as it is a key resource for image captioning and visual understanding tasks. It contains over 2.6 million training examples and over 12,000 test examples, with a wide range of web-sourced images, each paired with a descriptive caption.

OK-VQA We include the OK-VQA dataset (Marino et al., 2019) because it is an essential resource for visual question answering tasks that focus on the intersection of visual perception and knowledge-based reasoning. With over 14,000 samples, it contains a wide range of images, each associated with questions that require not only visual understanding, but also external knowledge for an accurate answer.

Wikipedia The Wikipedia dataset, built from the Wikipedia dump (Foundation), contains over 6 million English language samples as of March 1, 2022. It offers a wide range of topics and a wealth of information. By using this dataset, we aim to improve the language processing capabilities of our model and provide access to extensive reservoir of encyclopedic knowledge.

[5] Its original version from 2019: `https://huggingface.co/datasets/oscar`

C Image captioning additional examples

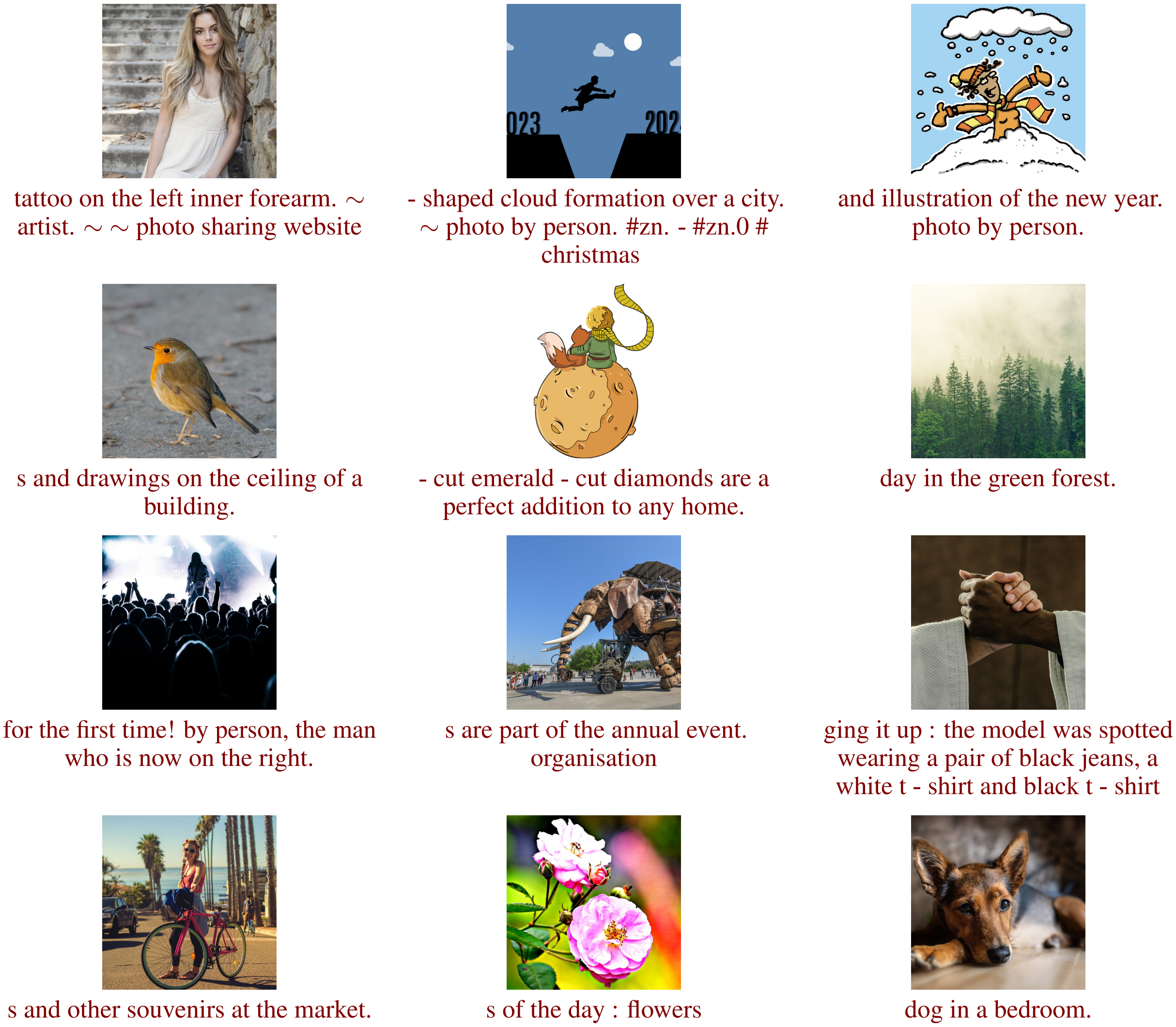

tattoo on the left inner forearm. ∼ artist. ∼ ∼ photo sharing website

- shaped cloud formation over a city. ∼ photo by person. #zn. - #zn.0 # christmas

and illustration of the new year. photo by person.

s and drawings on the ceiling of a building.

- cut emerald - cut diamonds are a perfect addition to any home.

day in the green forest.

for the first time! by person, the man who is now on the right.

s are part of the annual event. organisation

ging it up : the model was spotted wearing a pair of black jeans, a white t - shirt and black t - shirt

s and other souvenirs at the market.

s of the day : flowers

dog in a bedroom.

Figure 16: JAT image captioning additional examples.

D Reward as a Task Determinant

In multi-task learning, different environments may share identical dynamics and observational structures while differing in their ultimate goals (i.e., reward functions). Initially, the agent cannot distinguish the specific task it is facing. In most cases, this problem does not arise. For BabyAI, for example, the goal is an explicit part of the observation. For Atari, a single frame is sufficient to determine the game, and therefore the goal. In our dataset, the only domain that could be challenging in this respect is Meta-World, for which the structure of observations and dynamics is consistent across tasks. Note also that even in this case, it should be possible for the agent in some instances to infer the task from the initial conditions. We confirm this hypothesis in the following experiment.

To solve the problem of task indeterminacy, Gato introduces a method of pre-empting the sequence with an expert demonstration (prompt) to guide the agent. While this approach is effective, it imposes an important limitation: a demonstration must be available, and this demonstration must be sufficiently complete to clearly define the task. In the JAT model, we adopt a less restrictive and simpler approach by incorporating the reward signal directly into the observation encoding. We believe that this integration can, in most cases, provide the agent with sufficient context to remove ambiguity about the task at hand.

To support our hypothesis on the effectiveness of integrating reward signals into observations, we conducted an experiment with three different settings. First, to create a baseline where task indeterminacy is absent, we trained individual agents, each on a specific task from a random subset of 10 Meta-World tasks. This single-task training ensures that each agent is perfectly matched to its respective task, without any ambiguity. Next, we introduced a degree of indeterminacy by training a single model on the same 10 tasks without access to the reward signal, presenting a scenario that simulates a worst-case uncertainty condition. We compare these two settings with our full JAT model, i.e. with access to the reward signal, trained on the same selection of tasks. We compared the performance of these three scenarios, with the results detailed in Figures 17 following the recommendations of (Agarwal et al., 2021).

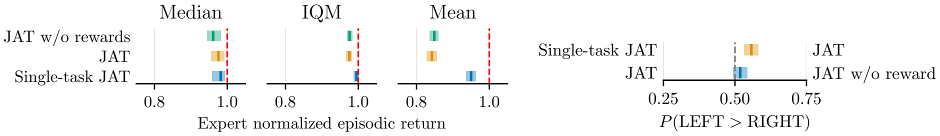

(a) Aggregated metrics.

(b) Probability of improvement.

Figure 17: Results of the reward ablation. The vertical bars are the estimated values and the shaded areas are the 95% stratified bootstrap CIs. The experiments were conducted on a selection of 10 tasks from the Meta-World benchmark. Displayed are the results of an ablation study on our JAT model variations: Single-task JAT with each task learned by a dedicated agent; JAT without rewards where the training omits reward signals; and the full JAT model integrating reward signals. Results are based on 100 evaluations per task.

Firstly, it's notable that the JAT model trained on a single task surpasses other settings, thus demonstrating the existence of a negative impact of task indeterminacy. However, this impact is actually very minor, and even in the most unfavorable setting (JAT without reward), the normalized IQM score reaches 97.6 ± 0.7%. This confirms the previously formulated intuition that the task can generally be inferred from the initial conditions. Then, when comparing the JAT model with and without access to the reward, we observe a probability of improvement from the former over the latter of 51.8 ± 2.5%, indicating that the addition of the reward has a significant, albeit small, positive effect on resolving indeterminacy. Lastly, the most significant gap is observed in the average score. This can be attributed to the fact that this metric accounts for outliers. Here, the outliers are the tasks suffering from indeterminacy, for which the agent often fails to resolve the task.

In summary, the key insight from this study is that complex solutions like prompting are often not required to address this task indetermination issue, as it typically presents a minimal challenge. Furthermore, in instances where the problem does manifest, implementing a straightforward strategy like incorporating the reward into the observation proves to be an effective measure for mitigation.